Quantifying the potential impacts of land-use and climate change on hydropower reliability of Muzizi hydropower plant, Uganda

Hilary Keneth Bahati, Abraham Ogenrwoth and Jotham Ivan Sempewo

ABSTRACT

Ugandan rivers are being tapped as a resource for the generation of hydropower in addition to other uses. Studies on the reliability of these hydropower plants due to climate and land-use/land cover changes on the hydrology of these rivers are scanty. Therefore, this study aimed to model the impact of the changing climate and land-use/cover on hydropower reliability to aid proper planning and management. The hydropower reliability of Muzizi River catchment was determined from its past (1998–2010) and midcentury (2041–2060) discharge at 30 and 95% exceedance probability under Representative Concentration Pathways (RCPs) of 4.5 and 8.5, respectively. The past and projected hydropower were compared to determine how future climate and land-use changes will impact the discharge and hydropower reliability of Muzizi River catchment. Six LULC scenarios (deforestation, 31–20%; grassland, 19–3%; cropland, 50–77%; water bodies, 0.02–0.01%; settlement, 0.23–0.37%, and Barren land 0.055–0.046% between 2014 and 2060) and three downscaled Regional Climate Model (REMO and RCA4 for precipitation and RACMO22T for temperature from a pool of four CORDEX (Coordinated Regional Climate Downscaling Experiment) Africa RCMs) were examined. A calibrated SWAT simulation model was applied for the midcentury (2041–2060) period, and a potential change in hydropower energy in reference to mean daily flow (designflow $\geq$ 30% exceedance probability), firm flow (flow $\geq$ 95% exceedance probability), and mean annual flow was evaluated under the condition of altered runoff under RCP4.5 and RCP8.5 climate change scenarios for an average of REMO and RCA4 RCM. The future land use (2060) was projected using the MOLUSCE (Module for Land Use Change Evaluation) plugin in QGIS using CA-ANN. Three scenarios have been described in this study, including LULC change, climate change, and combined (climate and LULC change). The results suggest that there will be a significant increase in annual hydropower generation capacity (from 386.27 and 488.1 GWh to 867.82 and 862.53 GWh under RCP4.5 and RCP8.5, respectively) for the combined future effect of climate and land-use/cover changes. Energy utilities need to put in place mechanisms to effectively manage, operate, and maintain the hydropower plant amidst climate and land-use change impacts, to ensure reliability at all times.

Key words | flow duration curves, hydropower potential, land-use change, RCP, SWAT-Cup Sufi-2, SWAT model

Hilary Keneth Bahati
Jotham Ivan Sempewo (corresponding author)
Department of Civil and Environmental Engineering,
Makerere University,
P.O. Box 7062, Kampala,
Uganda
E-mail: *jsempewo@cedat.mak.ac.ug*; *jothamsempewo@yahoo.com*

Abraham Ogenrwoth
Department of Water Resources Engineering,
Busitema University,
P.O. Box 236, Tororo,
Uganda

doi: 10.2166/wcc.2021.273

HIGHLIGHTS

- Innovative approaches for hydrological modeling in data-scarce scenarios.
- The possibility to utilize bias-corrected reanalysis and historical discharge data to build a climate model in data-scarce scenarios.
- Sheds light on the potential risks of land-use and climate change on hydropower reliability in data scarcity areas.
- Informs the need to implement prudent catchment management practices and develop policies.

INTRODUCTION

Hydropower is a key renewable energy source widely used as a driving force to power economic development and technological, scientific, anthropogenic, and industrial transformation in many countries across the world (Hwang & Yoo 2016). Currently, hydropower accounts for 86% of renewable energy technology that represents 16% (3,551 TWh/a) of global electricity generation which is projected to increase by 1% by 2050 (Hamududu & Killingtveit 2012). Global installed and electricity generated from hydropower in 2017 were 1,267 GW and 4,185 TWh, respectively (IHA 2018). Africa and Uganda represented 35.3 GW and 743 MW of the installed capacity, respectively.

Compared to other sources of renewable energy, hydropower is preferred because it is economical, reliable, and has low operation and maintenance costs. Like many other countries, Uganda relies on hydropower for 84% of its total installed capacity of 822 MW (Ministry of Energy & Minerals Development 2015). Recently, Uganda has embarked on a drive to increase its hydropower production which is mainly generated from the 255 MW Bujagali, the 200 MW Kiira, and the 180 MW Nalubaale plants by developing new hydropower plants (Rugumayo *et al.* 2014).

Despite being the main renewable energy source in the developing countries and sub-Saharan countries in particular (Cole *et al.* 2014; Falchetta *et al.* 2019), it is affected by climate and land-use change and their associated impacts (Hamududu & Killingtveit 2012; Puno *et al.* 2016; Falchetta *et al.* 2020). Accordingly, many studies have been carried out assessing the impacts of climate change on river flows (Todd *et al.* 2011; Hagemann *et al.* 2013; Roudier *et al.* 2014; Al-Safi & Sarukkalige 2017; Langat *et al.* 2017; Banze *et al.* 2018; Jin *et al.* 2018; Lv *et al.* 2019; Näschen *et al.* 2019; Pokhrel *et al.* 2019; Ndhlovu & Woyessa 2020) and land use on river flow (Bosmans *et al.* 2016; Zhang *et al.* 2016; Khare *et al.* 2017; Welde & Gebremariam 2017).

Most of the studies focused on the global or regional impact of climate change on hydropower which ignores catchment-specific variations within a region (Hamududu & Killingtveit 2012, 2010; Falchetta *et al.* 2019). Also, the few available studies within East Africa mainly looked at the individual impact of either climate change (Kizza *et al.* 2009; Conway *et al.* 2017) or land-use change (Khare *et al.* 2017) on hydropower production. This study notes that fewer studies have been undertaken on the combined impact of climate and land-use change on hydropower reliability within the East African Region, and as far as the Muzizi River catchment is concerned, the information regarding land use, climate changes, and hydropower production is scanty. Therefore, catchment-specific studies are required to inform decision-making (Hamududu & Killingtveit 2010).

Hydropower reliability (Lofthouse *et al.* 2011) is regarded as physical where the hydropower plant can consistently meet the demands of the users without any intermittency where there are fewer negative environmental impacts as compared to the fuels, or economical where the hydropower plant is economically viable, cost-effective, competitive, and sustainable without government subsidization. The physical reliability metrics concerning land-use and climate changes include the discharge potential, efficiency, and consistency to meet the demand. The environmental metrics include the hydropower plant's ability to not only work without

fuels that emit dangerous gases but also reduce the sediment accumulation, and economic reliability metrics include the hydropower plants' self-sustainability, leading to its viability and compatibility irrespective of the effects of land-use and climate changes.

This study has determined the land-use/land cover trends in the Muzizi River Catchment for the past 30 years (1984–2014) and projected the land-use and climate changes for the midcentury of the future (2040–2070), which estimates the design period of Muzizi hydropower plant. The Soil and Water Assessment Tool (SWAT) was employed to simulate the future potential impacts of land-use and climate changes on the Muzizi River catchment which is a resource that determines the reliability of the Muzizi Hydropower plant. The SWAT is an efficient, flexible, and continuous-time model that uses readily available data (Arnold *et al.* 2012). Developing countries including Uganda are vulnerable to the detrimental impacts of land-use and climate changes on hydropower reliability. Therefore, such a modeling analysis could support energy utilities in the planning and management of hydropower plants and their water resources.

DATA AND METHODS

Description of the study area

Muzizi Hydropower Plant is a planned 44.7 MW run-of-river hydropower plant on Muzizi River, located in Western Uganda, and about 6 km upstream of lake Albert, at the eastern flank of the Albertine Graben. It drops at an elevation of 900 m above sea level to 600 m for a distance of 3.5 km steep valley. The proposed project location is 0°56′56″N, 30°33′28″E in the Ndaiga sub-county of Kagadi district in Mid-Western Uganda. The 120 km-long Muzizi River starts in the Mubende district at an altitude of 1300 m and enters Lake Albert at an altitude of 620 m above sea level. The river forms the borders of Mubende, Kyegegwa, Kibaale, Kyenjojo, Kabarole, Kibaale, and Kagadi and Ntoroko Districts in the Muzizi River catchment of the Albert Water Management Zone (Figure 1). The Muzizi River catchment has a tropical climate that consists of both wet (March to May and September to November) and dry (December to February and June to August) seasons. Rainfall is bimodal

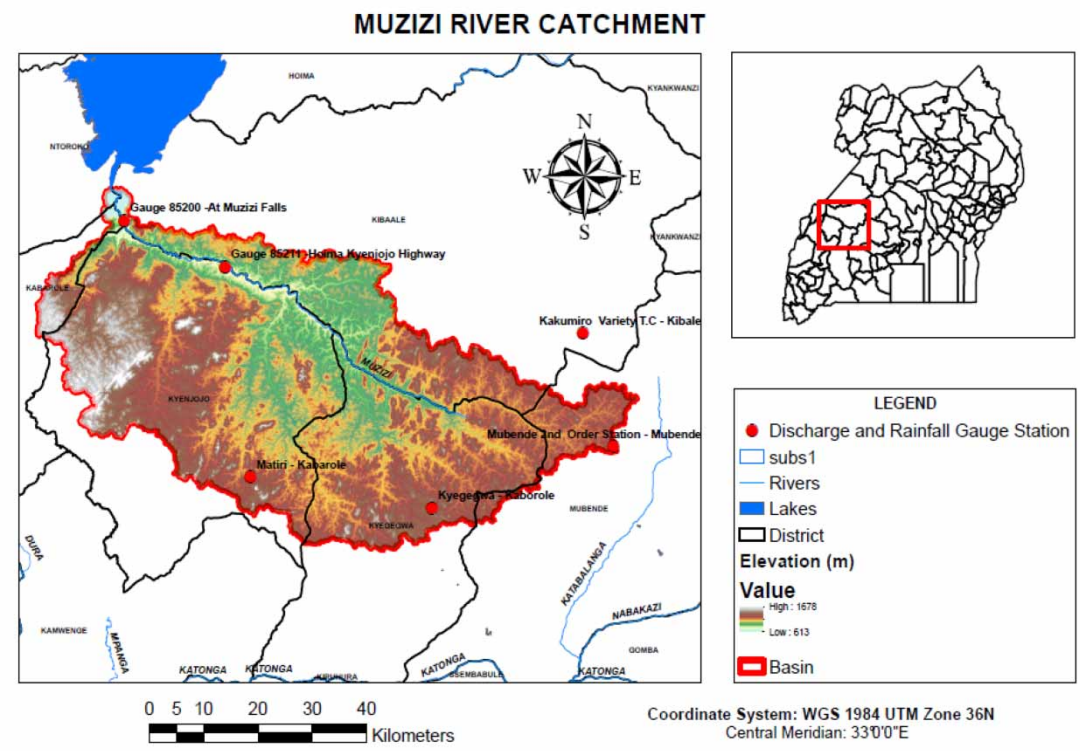

Figure 1 | The geographical location of the Muzizi Hydropower Station in Muzizi River catchment.

with a mean annual average of 700 mm at the mouth and 1300 mm at the source of the river. The temperature in the catchment ranges from 15.8 to 33 °C within the year.

Soil in the Muzizi River catchment is mapped according to three major districts that it borders. Kibaale district has granitic soils which are classified as shallow loams with moderated acidity, red clay loams, and brown gravelly clay loams. Kabarole district mainly has 90% black loams and red sandy clay loams (volcanic soils), while Kyenjonjo district has ferralsols, nitosols, kaolinite quartz, and iron oxides.

The relief of the Muzizi River catchment mainly consists of an undulating plateau traversed by valleys through which the river flows. The topography upstream of the project site is hilly with gentle slopes while approaching the Albertine Graben the terrain descends over an escarpment (UEGCL 2013a). The land-use/cover of the Muzizi River catchment is dominated by agriculture and vegetation. The 17,151 ha Kagombe Central Forest Reserve in the catchment plays a significant role in its hydrology. The built-up areas of the settlement are also increasing partly because of immigration of people from other districts and inflows of refugees from the Democratic Republic of Congo.

Data sources

The SWAT model uses readily available input data such as digital elevation model (DEM), land-use data, soil data, and climatic data, and the functions are summarized in Table 1.

Digital elevation model

The DEM allows ease of identification and measurement of the surface drainage area of catchment, which is among the first steps in conducting catchment delineation. The DEM for Uganda of 30 m-by-30 m resolution has been downloaded from the USGS website (http://gdex.cr.usgs.gov/gdex/). The DEM for the Muzizi River catchment was clipped from the DEM of Uganda using its catchment boundaries. The DEM was used for catchment delineation, analysis of drainage patterns, and land surface characteristics. The Muzizi Catchment DEM was clipped from the DEM of Uganda using its catchment boundaries and with the help of the ArcGIS-based Clip tool.

Soil data

Soil types and land cover type are vital in determining the catchment surface runoff. Curve Number Soil data for the Muzizi River catchment was extracted using the sub-catchment boundary from the Food and Agriculture Organization (FAO) harmonized soil database of Africa downloaded from http://www.fao.org/soils-portal/soil-survey/soil-maps-and-databases/harmonized-world-soil-

Table 1 | The data used for model setup

Data type	Description	Scale	Data source
Digital elevation models	For delineation of the watershed and define hydrological response unit	30 m	http://gdex.cr.usgs.gov/gdex/.
Land-use/land cover map	Used in the SCS CN method in SWAT, and projection for future land use	300 m	Remotely sensed downloads: United States Geological Survey website (http://glovis.usgs.gov/)
Soil data–Uganda soil map	Generates a curve number map	10 km	http://www.fao.org/soils-portal/soil-survey/soil-maps-and-databases/harmonized-world-soil-database-v12/en.
Hydro-meteorological data	Necessary for model calibration	Daily and monthly	DWRM, Ministry of Water and Environment
	Streamflow	Daily and monthly	DWRM, Ministry of Water and Environment, Uganda.
Climate data	Daily rainfall and temperature, dew point, wind speed, and relative humidity	Daily	Uganda National Meteorological Authority, Office of the Prime Minister, Uganda https://globalweather.tamu.edu/

database-v12/en. The attributes of the soils were updated using a user soil table in SWAT vital for SWAT run.

Land-use/cover data

Remotely sensed land-use/cover data of the Muzizi River catchment for the years of 1984, 2000, and 2014 were downloaded from the United States Geological Survey website (http://www.earthexplorer.usgs.gov/) (USGS, 2020) from two paths and rows (path172/row059 and path172/row060). The downloaded images were of less than 10% cloud cover and 30 m spatial resolution.

The images were classified into six land-use/cover types in accordance with Anderson *et al.*'s (1976) Level I generalized classification system using the maximum likelihood supervised classification tool in ArcGIS. These are settlement area, water bodies, forestland, crop/agricultural land, grassland, and bare land.

Hydro-meteorological data

Daily rainfall and temperature data for the Muzizi River catchment from 1980 to 2010 were obtained from the Uganda National Meteorological Authority (UNMA). Other climate variables for SWAT modeling were obtained from https://globalweather.tamu.edu/. Daily discharge data for the Muzizi River catchment at Kyenjojo-Hoima road gauging station were obtained from the Directorate of Water Resources Management (DWRM), Ministry of Water and Environment, Uganda. The observed discharge data were used for model calibration and validation. Figure 1 shows the locations of the climatological stations overlaid.

Reanalysis precipitation data

ERA5, CFSR, CHIRPS, MERRA2, TRMM 3B42, and NASA Agro climatology, which are available to the public, were chosen, corrected for bias using the method proposed by Berhanu *et al.* (2016), and evaluated for suitability. Table 2 shows the six reanalysis precipitation data used in the evaluation of the observed data.

Gauged flow data

Muzizi Catchment river flow data were obtained from the DWRM, Ministry of Water & Environment, Uganda. Two gauge stations were identified for statistical analysis in mean annual flows, monthly flows, daily flows, maximum and minimum flows, and firm flow in the assessment of hydropower reliability of the river. Flow Gauge Station 85211 located on Muzizi River along Kyenjojo-Hoima highways presents flow data for the years 1956–2010. River discharge for years 1957–1977 and years 1998–2010 are considered reliable (with no missing gaps) in assessing the catchment current surface water resources and hydropower reliability. Flow Gauge Station 85200 just 20 km

Table 2 | Reanalysis precipitation data used in model evaluation

Acronym	Data period	Name and institute	Spatial resolution	Data source (website)
ERA5 Reanalysis	1979–2010	ERA5	24-km (0.25-deg × 0.25-deg)	https://www.ecmwf.int/en/forecasts/datasets/reanalysis-datasets/era-interim
CFSR Reanalysis	1979–2010	NCEP Climate Forecast System Reanalysis dataset	19.2-km (0.2-deg × 0.2-deg)	http://cfs.ncep.noaa.gov/cfsr/
CHIRPS	1980–2010	Climate Hazards Group (CHG) InfraRed Precipitation with Station data (CHIRPS)	4.8-km (0.05-deg × 0.05-deg)	https://www.chc.ucsb.edu/data/chirps
MERRA2 Reanalysis	1980–2010	Modern-Era Retrospective analysis for Research and Applications, Version 2	50-km (0.5-deg× 0.625-deg)	https://gmao.gsfc.nasa.gov/reanalysis/MERRA-2/
TRMM 3B42	1998–2010	Tropical Rainfall Measuring Mission 3B42	28-km (0.25-deg × 0.25-deg)	https://trmm.gsfc.nasa.gov/
NASA Agroclimatology	1981–2010	NASA Agroclimatology Centre	0.5-deg × 0.5-deg	https://power.larc.nasa.gov/data-access-viewer/

downstream of Gauge Station 85211 presents flow data for the period 2009–2018 with the only reliable data being from 2009 to 2015. The Muzizi Hydropower Dam is a few meters' distance downstream of Gauge Station 85200 impact assessment in this study. Hydrological modeling using the SWAT can be calibrated and validated based on flow Gauge Station 85211 data, while Gauge station 85200 flow shall be considered in assessing the hydropower reliability of Muzizi River.

Methodology

The main objective of this paper is to quantify the potential impacts of land-use and climate change on hydropower reliability. Details of the methodology are highlighted in the below sections.

Performance evaluation of reanalysis data

To fill in gaps for missing data, reanalysis of precipitation data which was widely applied by scholars in hydrological modeling was used. The reanalysis data in the section 'Reanalysis precipitation data' were first assessed to identify the most accurate reanalysis dataset that can better mimic observed data within the catchment. The performances of the reanalysis data were evaluated by comparing the gridded reanalysis data with the observed point/gauged climatic data. Given the two stations with continuous time series over the catchment, a point-pixel comparison was performed in this study to avoid errors by gridding the rain gauge data following (Li *et al.* 2013; Darand *et al.* 2017). Before comparison, ERA5, CFSR, CHIRPS, and TRMM 3B42 were resampled to horizontal $0.5^\circ \times 0.5^\circ$ grid scales to acquire a uniform spatial resolution by bilinear interpolation, which is a popular method in meteorology and climate studies (Hu *et al.* 2013; Zhu *et al.* 2015). However, considering the unequal spacing between x and y coordinates between the grid points of MERRA2 reanalysis data, resampling will introduce errors. Therefore, rain gauge data were directly compared against the nearest grid points of MERRA2 in the original resolution without resampling.

The quantitative assessment of the performance of the six reanalysis climate data in simulating observed mean monthly precipitation was undertaken using the following: (i) the Nash–Sutcliff efficiency (NSE) indicates the goodness of fit of the reanalysis data and observed data (Moriasi *et al.* 2007); (ii) the coefficient of determination (R^2) describes the proportion of the variance in the measured data (Santhi *et al.* 2001; Van Liew *et al.* 2003), and (iii) the root mean square error (RMSE) assesses how perfect the match between observed and reanalysis data values are (Singh *et al.* 2004); (iv) PBIAS, the percentage of bias, measures the average tendency of the reanalysis data to be larger or smaller than the observed data; (v) Spearman rank correlation coefficient (R's) was used as the primary and principle indicator to evaluate the accuracy of precipitation products (Reanalysis) in estimating observed/gauged data as guided by Jiang *et al.* (2012) and Sun *et al.* (2014).

A t-test was carried out at a 5% (α) level of significance to estimate the P-value to assess the reliability of the null hypothesis (H_0) which was formulated as follows: observed and reanalysis precipitation are not significantly different.

Reanalysis precipitation performance was judged by the magnitude of the statistical results of PBIAS, RMSE, Rs, R^2, and N and the ability of reanalysis precipitation in reproducing mean monthly, mean daily, and sum of monthly observed precipitation.

Bias correction of selected reanalysis precipitation

The best performing/selected reanalysis is a product containing historical (1981–2010) precipitation data, typically containing biases when compared with observations (Mehrotra & Sharma 2015). Bias correction was carried out to correct the historical precipitation using the differences in the mean and variability between reanalysis and observed datasets. In this study, the biases in the daily time series of the precipitation from the selected reanalysis output were corrected using the easiest and the most common method, which was the multiplicative method for precipitation (Ashraf Vaghefi *et al.* 2017; Krapp *et al.* 2019). Here, the multiplicative correction factor for each month was used, and the modified daily rainfall was expressed as in the equation below:

$$P_{corrected\,ij} = P_{GCM\,ij}\, X\, \frac{\bar{P}_{reference\,jk}}{\bar{P}_{GCM\,jk}} \quad (1)$$

where P is the precipitation (mm/day), $\bar{P}$ is the long-term average precipitation and i, j, k are the day, month, and year counters, respectively.

Projection of future land use and climate of Muzizi River catchment

Accuracy assessment of the remotely sensed/classified land-use/cover data

This was carried out to compare the classified image to/with another data source (in this case Google image) that is considered to be accurate or ground truth data.

In this study, the accuracy of classified images for 1984, 2000, and 2014 was performed by creating a set of random points (also known as the ground truth point) and compared them with the classified data in a confusion matrix. The random points were termed as users' points which represent classified image pixels, while producers' points were the equivalent of users' point land use in google images. Users' and producers' accuracy were calculated as shown in Equations (2) and (3), respectively. The overall accuracy was obtained as the sum of the correctly classified pixel divided by the total number of samples expressed as a percentage in Equation (4). While the statistical test of the classification accuracy for individual pixels was determined using the Kappa statistic (Equation (5)).

where TS is the total sample and TCS is the total corrected classified sample (diagonal).

The statistics have values ranging from 0 to 1 although negative values are possible but rare. K values closest to 1 indicate almost perfect agreement (Othow *et al.* 2017).

Muzizi catchment land-use validation and projection

A coupled Cellular Automata (CA)–Markov model is employed to conduct LULC change modeling in this study. A Markov chain is a stochastic model describing a sequence of possible events in which the probability of each event depends only on the state attained in the previous event (Gagniuc 2017). A countably infinite sequence, in which the chain moves state at discrete-time steps, gives a discrete-time Markov chain. A continuous-time process is called a continuous-time Markov chain. CA–Markov model combination represents an advancement in spatio-temporal dynamic modeling and forecasting, achieving a better simulation of LULC changes both in quantity and space. The algorithms in the MOLUSCE (Module for Land Use Change Evaluation) integrate the functions of the CA filter and Markov process using conversion tables and conditional probabilities from the conversion map applied to simulate and forecast the states of LULC change. Therefore, to simulate future LULC changes for our study site using a CA–Markov model, the following specific processes were followed.

$$\text{Users Accuracy} = \frac{\text{Number of Correctly Classified Pixels in Each Category}}{\text{Total Number of Classified Pixels in that Category (The Row Total)}} \times 100 \quad (2)$$

$$\text{Producer Accuracy} = \frac{\text{Number of Correctly Classified Pixels in Each Category}}{\text{Total Number of Classified Pixels in that Category (The Row Total)}} \times 100 \quad (3)$$

$$\text{Overall Accuracy} = \frac{\text{Total Number of Correctly Classified Pixels (Diagnol)}}{\text{Total Number of Sample Pixels}} \times 100 \quad (4)$$

$$\text{Kappa Coefficient}(T) = \frac{(\text{TS x TCS}) - \sum(\text{Column Total x Row Total})}{\text{TS}^2 - \sum(\text{Column Total x Row Total})} \times 100 \quad (5)$$

Generation of transition matrix

Accuracy assessed classified LULC maps for the years 1984, 2000, and 2014 were used to obtain the transition matrices for the LULC categories between 1984 and 2000 as well as 2000 and 2014 based on the first-order Markov model (Veldkamp & Lambin 2001; Fitzsimmons & Getoor 2003).

Model validation

To validate the model based on the CA–Markov model approach in MOLUSCE, transition potential modeling using the artificial neural network (ANN) model method was applied to simulate 2014 land-use/change using the transition probabilities/matrix from 1984 to 2000 with the LULC base map year 2000.

Kappa statistics were used to assess the accuracy of the forecasted/simulated 2014 LULC map to evaluate its agreement with the actual/reference 2014 LULC map. Kappa (hist), Kappa (loc), Kappa (overall), and percentage correctness determine the accuracy of simulated 2014 land use in reproducing reference 2014 land use. Kappa statistic close to value 1 and percentage correctness close to 100% indicate good ability of the model to project accurate future land-use/change. Therefore, the model is said to be validated.

Projection of Muzizi catchment future (2060) land use

After validation of the model, the LULC for the year 2060 was projected with the CA–Markov model in MOLUSCE using the transition probabilities from 1984 to 2000 and 2000 to 2014 and using the LULC base map from the year 2014.

Hydrological modeling

SWAT model and model setup

The SWAT is a physically-based, semi-distributed hydrological model that predicts the impact of land management practices on water, sediment, and agricultural chemical yields in large complex watersheds of varying soils, land-use/cover, and management conditions over long periods (Neitsch *et al.* 2011). The model simulates the hydrological cycle based on the water balance (Equation (6)).

$$\mathrm{SW}_t = \mathrm{SW}_o + \sum_{t=1}^{t} (R_i - Q_i - \mathrm{ET}_i - P_i - \mathrm{QR}_i) \quad (6)$$

where SW_t is the final soil water content and SW_o is the initial soil water content of the day i, t is time in days, and R, Q, ET, P, and QR are the daily amounts of precipitation, surface runoff, evapotranspiration, percolation, and return flow, respectively, all measured in mm. The model uses readily available input data such as DEM, land-use data, soil data, and climatic data as described in the section 'Data sources'. In this study, modeling of the hydrological process was carried out using the extension of SWAT for ArcGIS software called ArcSWAT (Anaba *et al.* 2017). ArcSWATv2012.10.1.18 was downloaded from the website for the model (http://swat.tamu.edu/software/arcswat/) and installed in ArcGISv10.5. In the model setup, the first step was to delineate the catchment using the DEM into several connected sub-basins. The sub-basins were further divided into smaller units called hydrologic response units (HRUs). HRUs have lumped land areas within the sub-basin that are comprised of unique land cover, soil, slope, and management combinations (Neitsch *et al.* 2011). A total of 27 sub-basins and 247 HRUs were created. The HRUs were created by defining the thresholds of land use over sub-basin area at 5%, soil class over land-use area at 5%, and slope class over soil area at 5% using the multiple HRU definitions. The model was run on a daily time step for a period of 8 years from 2002 to 2010 with a warm-up period of 3 years.

Sensitivity analysis

Sensitivity analysis was performed to choose the most sensitive flow parameters (Abbaspour *et al.* 2007) that influence the catchment represented by the SWAT to be used for calibration. This was achieved using the global sensitivity approach in the semi-automated Sequential Uncertainty Fitting (SUFI2) algorithm. The global sensitivity analysis method takes into consideration the sensitivity of one parameter relative to the other to give their statistical significances (Atkinson *et al.* 2010). The t-statistics and p-values of the parameters were used to rank the different parameters

considered to influence flow, and the final selection was done based on the significance of the ranked values.

Calibration and validation of the model

Calibration was accomplished by comparing the output of the SWAT model with the observed data at the same conditions (Engel *et al.* 2007; Arnold *et al.* 2012). For calibration and validation, the semi-automated Sequential Uncertainty Fitting (SUFI-2) calibration method within the SWAT Calibration and Uncertainty Procedures (SWAT-CUP) was used. The SWAT-CUP version 5.1.6.2 was used (Anaba *et al.* 2017). SWAT-CUP is a stand-alone calibration program developed for SWAT that operates on Latin Hypercube sampling procedures. Due to a lack of observed data for sediment and nutrients, the model was calibrated and validated only for streamflow. The model was calibrated with observed daily discharge data for the period of 2002–2007 and validated from 2008 to 2010. Though there were gaps in the observed data, the challenge was addressed by writing it in a format suggested by Abbaspour *et al.* (2015) that the SWAT-CUP tool can read.

Evaluation of model performance

To evaluate the performance of the model during calibration and validation, statistical measures, as well as graphical representations at a daily time step, were used. This was employed to confirm the relationship between simulated or predicted values and observed values (Ndulue *et al.* 2015) and to verify the robustness of the model (Betrie *et al.* 2011). Three statistical measures were employed. They are the coefficient of determination, R^2 (Equation (7)), the NSE (Equation (8)), and the PBIAS (Equation (9)). Other details of these measures such as their utility and satisfactory range of values are explained by Moriasi *et al.* (2007).

$$R^2 = \frac{\sum_{i=1}^{n}(O_i - \bar{O})(P_i - \bar{P})}{\sqrt{\sum_{i=1}^{n}(O_i - \bar{O})^2}\sqrt{\sum_{i=1}^{n}(P_i - \bar{P})^2}} \tag{7}$$

$$\text{NSE} = \frac{\sum_{i=1}^{n}(O_i - \bar{O})^2 - \sum_{i=1}^{n}(P_i - O_i)^2}{\sum_{i=1}^{n}(O_i - \bar{O})^2} \tag{8}$$

$$\text{PBIAS} = \frac{\sum_{i=1}^{n}(O_i - P_i) \times 100}{\sum_{i=1}^{n}(O_i)} \tag{9}$$

where n is the number of observations in the period under consideration, O_i is the ith observed flow, $\bar{O}$ is the mean observed value, P_i is the ith simulated flow, and $\bar{P}$ is the mean of simulated flow.

Evaluation of the performance of GCMs in simulating current climate conditions of Muzizi River catchment

Brief introduction

Information obtained from global climate models (GCMs) supports a better understanding of the climate at a global scale. The output from GCMs is too coarse (>100 km) to be used in impact assessment studies, adaptation planning, and decision-making processes at a local or regional scale (Treesa *et al.* 2017). In addition to the coarse resolution, biases and uncertainties associated with GCMs increase from global to regional and local scales, which limit the suitability and applicability of GCMs in local-scale impact assessment studies (Bayar & Özel 2014; Gebrechorkos *et al.* 2019). Therefore, downscaling is required to increase the spatial resolution and reduce biases (Gebrechorkos *et al.* 2019) before climate projections can be used for impact assessment and adaptation planning. In this study, GCMs simulation was downscaled to station scale using Delta adjustment bias correction techniques of precipitation and temperature. The downscaling process was as follows.

GCM performance/evaluation

Model data. The Coordinated Regional Climate Downscaling Experiment (CORDEX) program archives output from a set of RCM simulations over different regions in the world. The CORDEX domains for model integrations are found at http://wcrp-cordex.ipsl.jussieu.fr/images/pdf/cordex_regions.pdf. In this study, datasets from CORDEX Africa were accessed from http://cordexesg.dmi.dk/esgf-web-fe/. The dataset was downloaded for the historical (1971–2005)

period (for precipitation, minimum, and maximum temperature) and midcentury (2040–2060) period for RCP4.5 and RCP8.5. Climate change scenario 4.5 was chosen because it is an intermediate pathway scenario that shows a good agreement with the latest policy of lower greenhouse gas emissions by the global community, while RCP8.5 is the business-as-usual scenario, which is consistent with a future that has no change in climate policy to reduce emissions (Wang *et al.* 2017). CORDEX datasets are quality controlled and may be used according to the terms of use (http://wcrp-cordex.ipsl.jussieu.fr/). The spatial grid resolutions of all CORDEX-Africa RCMs were set to longitude 0.44° and latitude 0.44° using a rotated pole system coordinate. These models operate over an equatorial domain with a quasi-uniform resolution of approximately 50 km by 50 km. For a detailed description of CORDEX-RCMs and their dynamics and physical parameterization consult, see Wang *et al.* (2017). Table 3 lists the details of CORDEX-RCMs and the driving GCMs: MOH-HadGEM2-ES,MPI-M-MPI-ESM-LR, and ICHEC-EC-EARTH.

The output from CORDEX-RCMs driven by boundary conditions from the GCMs for the period of 1971–2005 was used to assess the ability of the RCMs to simulate mean monthly, daily, mean annual cycle of rainfall, minimum temperature, and maximum temperature the same way as done in another study by Masanganise *et al.* (2013) under an evaluation of the performances of GCMs for predicting temperature and rainfall in Zimbabwe, and Luhunga *et al.* (2016) under evaluation of the performance of CORDEX regional climate models in simulating present climate conditions of Tanzania.

Observed data. The bias-corrected CHIRPS-driven simulations which are available for the period of 1981–2010 are used to assess the ability of CORDEX-RCMs to simulate mean monthly, mean daily, and mean annual cycle in rainfall and minimum and maximum temperatures.

Evaluation criteria. The ability of RCMs to simulate climate conditions at a particular location can be evaluated using a variety of techniques (Masanganise *et al.* 2013). However, no individual evaluation technique or performance measure is considered superior; rather, it is combined use of many techniques and measures that provides a comprehensive overview of model performance (Masanganise *et al.* 2013). In this study, outputs from RCMs are evaluated against observations using some of the statistical measures recommended by the World Meteorological Organization (WMO) as reported in Gordon & Shaykewich (2009) and as per Masanganise *et al.* (2013). These statistics include PBIAS, RMSE, Pearson's correlation coefficient (*R*s), coefficient of determination (R^2), and NSE.

The output from CORDEX-RCMs was compared with observed precipitation and temperature over the full period (1981–2005) from different stations in the catchment. Observed precipitation, in this case, was the bias-corrected CHIRPS reanalysis data. Observed minimum and maximum temperatures for the same period (1981–2005) for the Muzizi catchment, calculated as the arithmetic mean of all six weather stations, were compared with the outputs from the RCMs to determine how well the RCMs were driven by GCMs capture temperature.

Table 3 | Details of CORDEX-RCMs and the driving GCMs

No.	RCM	Model center	Short name of RCM	Driving GCM
1	CLMcom COSMO-CLM (CCLM4)	Climate Limited-Area Modelling (CLM) Community	CCLM4	MOH-HadGEM2-ES
2	MPI-CSC-REMO2009	Helmholtz-ZentrumGeesthacht, Climate Service Center, Max Planck Institute for Meteorology	REMO2009	MPI-M-MPI-ESM-LR
3	SMHI Rossby Center Regional Atmospheric Model (RCA4)	Sveriges Meteorologicaloch HydrologiskaInstitute (SMHI), Sweden	RCA4	ICHEC-EC-EARTH
4	KNMI Regional Atmospheric Climate Model, version 2.2 (RACMO2.2 T)	KoninklijkNederlandsMeteorologischInstitute (KNMI), Netherlands	RACMO22T	ICHEC-EC-EARTH

A *t*-test was carried out at 5% (α) level of significance to estimate *P*-value to assess the reliability of the null hypothesis (H_0), which was formulated as follows: observed and simulated data are not significantly different. A two-tailed test (Equation (10)) was performed for each pair of datasets after the estimation of their Spearman rank correlation coefficient (Equation (9)). The null hypothesis was rejected when the *p*-value obtained was greater than α-critical (0.05). That is, H_0 was rejected when *p*-value was >0.05; otherwise, it was not rejected. Model performance was judged by the magnitude of the statistical results of PBIAS, RMSE, *Rs*, R^2, and NSE.

$$t = \frac{IRsI\ X\ \sqrt{n-2}}{\sqrt{1-IRsI^2}} \tag{10}$$

where *IRsI* is the absolute value of Spearman rank correlation coefficient *Rs* and *n* is the number of data (samples). *P*-value was estimated using the TDIST command in Microsoft excel after the calculation of the degree of freedom (DF = $n-2$).

Climate change data bias correction/downscaling

Climate model data for hydrologic modeling (CMhyd) was used to extract and bias correct the best-selected RCM model outputs and provide climate data for the SWAT model (Rathjens *et al.* 2016). Precipitation and temperature data were bias corrected using the Delta adjustment correction techniques method available in the CMhyd software. Best-selected reanalysis precipitation data and CFRS temperature of the catchment were used for the bias correction of the RCM climate data.

Assessment of Muzizi current water resources and hydropower reliability

Flow duration curve

The current/reference flow (water availability) of the Muzizi River catchment was determined from the dependable discharges that correspond to 95% exceedance probability (Equation (6)), herein considered as a firm flow (https://hydroco.ca/glossary/firm-flow/). The firm discharge is the discharge that can be exclusively used for hydropower generation almost every day of the year. It ranges from flow corresponding to 90–95% exceedance probability (Japan International Cooperation Agency, 2011). The firm flow was determined from flow duration curve (FDC) analyses which estimate the percentage of time that a specified flow is equaled or exceeded during a given period (Searcy, 1959). FDC is estimated by sorting the daily mean flows for the period of record from the largest value to the smallest value and assigning flow value a rank from 1 to the largest value. The frequencies of exceedance are then computed using the Weibull formula for computing plotting position.

$$p = \frac{m}{n+1} \tag{11}$$

where *p* is the probability that a given flow will be equaled or exceeded (percentage of the time)

m is the ranked position (dimensionless), and

n is the number of events for the period of record (dimensionless).

Flow duration analysis for this report was estimated using the above equation and plotted graphically as represented hereafter.

To be consistent with low-flow statistics, flow durations were computed based on daily mean flows available through 1998–2012, with 14 full years of data. The flow duration curve constructed for daily time series enables a detailed examination of the flow duration characteristics of the Muzizi River.

Muzizi River current hydropower reliability

The current reliability (firm capacity) of hydropower of the Muzizi River catchment was calculated using Equation (3) (Hasan & Wyseure 2018) for the obtained firm discharges corresponding to 95% exceedance probability. The firm discharge was obtained from resultant FDC after subtraction of environmental flow from all values of the flow duration curve. The Ministry of Water and Environment of Uganda recommends a minimum of 0.69 m^3 /s of water to be maintained downstream as an environmental flow after abstraction for hydropower power production.

$$P = \eta\rho gQH \tag{12}$$

where P is power (MW), η is the average total turbine efficiency, ρ is water density (kg/m^3), Q is discharged (m^3/s), g is gravity (9.81 m/s^2), and H is the hydraulic head (m). In this study, the average total turbine efficiency was determined as 87%, as an average resultant efficiency of the 90.4% constant Pelton turbine efficiency proposed to be used at Muzizi Hydropower plant, 97% of the generator efficiency, and 99% of the transformer efficiency. The net head is considered as 459.3 m as it is the net difference between the reservoir full supply and the minimum operational level less hydraulic loss 7 (Hasan & Wyseure, 2018).

The current Muzizi installed capacity of hydropower was estimated using Equation (11) based on the historical average daily (for river flows for the period of 1998–2012 excluding missing data) flow herein considered as design/optimum discharge. This corresponds to exceedance probability in the range of 26–30% on the flow duration curve similar to that estimated by UEGCL (2013b) (see also Uamusse *et al.* 2017).

RESULTS AND DISCUSSION

Performance of reanalysis precipitation

The results of the performance assessment of the six different reanalysis datasets with respect to simulating mean monthly, mean daily, and mean annual precipitation for the period of 1981–2010 as compared to their respective observed precipitation are shown in Tables 4–6, respectively.

The results show that overall CHIRPS data outperformed other datasets in simulating mean monthly, mean daily, and mean annual precipitation for the period of 1981–2010 as compared to their respective observed precipitation. CHIRPS reanalysis precipitation was adopted throughout the study in assessing the impact of climate and land-use change onto Muzizi HPP reliability.

Muzizi catchment land-use/cover classification

Land-use accuracy assessment

Table 7 shows the accuracies and Kappa coefficient for the land-use/cover classifications for Muzizi River catchment in 1984, 2000, and 2014, respectively.

Accuracy assessed land use

The results show that forest land area coverage increases to 41.48% in 2000 from 29.15% in 1984 (Table 8). However, the forested areas declined to 31.12% of the total catchment area in 2014. Cropland and settlement area have increased to 50.02 and 0.23%, respectively, in 2014 as compared to the 8.6 and 0.01% in the year 1984. The increase in

Table 4 | Performance of reanalysis data concerning simulating observed mean monthly precipitation

		Reanalysis rainfall (mean monthly precipitation)					
Statistic	**Observed station**	**ERA5 Reanalysis (1979–2010)**	**CFSR Reanalysis (1979–2010)**	**CHIRPS (1980–2010)**	**MERRA2 Reanalysis (1980–2010)**	**TRMM 3B42 (1998–2010)**	**NASA Agroclimatology (1981–2010)**
R^2	Matiri	0.75	0.76	**0.84**	0.81	0.69	0.78
	Kakumiro	0.85	0.58	**0.88**	0.82	*	0.58
PBIAS	Matiri	−0.18	0.68	**0.04**	−0.16	0.13	−0.072
	Kakumiro	−0.40	0.58	**− 0.17**	−0.42	*	−0.338
RMSE	Matiri	24.90	61.94	**13.81**	21.03	4.72	16.408
	Kakumiro	13.09	18.20	**4.51**	8.90	*	6.450
NSE (%)	Matiri	0.60	−1.45	**0.83**	0.69	0.64	0.758
	Kakumiro	−0.42	−1.75	**0.72**	−0.10	*	0.625
*R*s	Matiri	0.86	0.79	**0.91**	0.91	0.84	0.818
	Kakumiro	0.90	0.74	**0.94**	0.83	*	0.888
p-value	Matiri	0.00033	0.00222	**0.00004**	0.00004	0.00064	0.00114
	Kakumiro	0.00006	0.00580	**0.00001**	0.00095	*	0.00011

*Missing.
Best evaluated reanalysis dataset selected to drive hydrological modelling.

Table 5 | Performance of reanalysis data concerning simulating observed mean daily precipitation in a month

		Reanalysis rainfall (mean daily)					
Statistic	**Observed station**	**ERA5 Reanalysis (1979–2010)**	**CFSR Reanalysis (1979–2010)**	**CHIRPS (1980–2010)**	**MERRA2 Reanalysis (1980–2010)**	**TRMM 3B42 (1998–2010)**	**NASA Agroclimatology (1981–2010)**
R^2	Matiri	0.76	0.77	**0.83**	0.78	0.52	0.73
	Kakumiro	0.85	0.64	**0.96**	0.79	*	0.81
PBIAS	Matiri	−0.18	0.68	**0.04**	−0.10	0.07	−0.08
	Kakumiro	−0.40	0.58	**− 0.16**	−0.42	*	−0.35
RMSE	Matiri	1.05	2.59	**0.71**	0.90	1.38	0.90
	Kakumiro	1.40	1.92	**0.80**	1.61	*	1.35
NSE	Matiri	0.61	−1.39	**0.83**	0.74	0.49	0.71
(%)	Kakumiro	−0.48	−1.79	**0.69**	−0.26	*	0.85
*R*s	Matiri	0.91	0.78	**0.92**	0.86	0.66	0.84
	Kakumiro	0.84	0.80	**0.96**	0.84	*	0.85
p-value	Matiri	0.00004	0.00299	**0.00003**	0.00033	0.01845	0.00064
	Kakumiro	0.00064	0.00190	**0.00000**	0.00064	*	0.00052

*Missing.
Best evaluated reanalysis dataset selected to drive hydrological modelling.

Table 6 | Performance of reanalysis data with respect to simulating observed mean annual precipitation

		Reanalysis rainfall (mean annual precipitation)					
Statistic	**Observed station**	**ERA5 Reanalysis (1979–2010)**	**CFSR Reanalysis (1979–2010)**	**CHIRPS (1980–2010)**	**MERRA2 Reanalysis (1980–2010)**	**TRMM 3B42 (1998–2010)**	**NASA Agroclimatology (1981–2010)**
R^2	Matiri	0.75	0.76	**0.84**	0.81	0.69	0.78
	Kakumiro	0.85	0.58	**0.88**	0.82	*	0.58
PBIAS	Matiri	−0.18	0.68	**0.04**	−0.16	0.13	−0.07
	Kakumiro	−0.40	0.58	**− 0.17**	−0.42	*	−0.34
RMSE	Matiri	398.46	991.03	**220.92**	336.54	75.50	262.52
	Kakumiro	209.50	291.12	**72.13**	142.32	*	103.19
NSE (%)	Matiri	0.60	−1.45	**0.83**	0.69	0.64	0.76
	Kakumiro	−0.42	−1.75	**0.72**	−0.10	*	0.46
*R*s	Matiri	0.86	0.79	**0.91**	0.91	0.84	0.82
	Kakumiro	0.85	0.74	**0.94**	0.83	*	0.89
p-value	Matiri	0.00033	0.00222	**0.00004**	0.00004	0.0006	0.00114
	Kakumiro	0.00006	0.00580	**0.00001**	0.00095	*	0.0001

*Missing.
Best evaluated reanalysis dataset selected to drive hydrological modelling.

Table 7 | Overall accuracies and Kappa coefficient for the classified land use

Land use	**1984**	**2000**	**2014**
Overall accuracies (%)	75.00	81.25	87.50
Kappa coefficient	0.67	0.75	0.84

Classified land use was deemed accurate, given their Kappa coefficient values being closer to 1.

land-use/cover of farmland and settlement from 1984–2014 was because of the need to produce more food and built houses for the ever-increasing population in the catchment. The increase in the area coverage of forest land between 1984 and 2000 was attributed to the good environmental policies that had been set by the new government which had been ushered in, within that period, which was restricting

Table 8 | Reference and projected land-use/cover of Muzizi River catchment for the year of 2060

	Year 1984		Year 2000		Year 2014		Year 2060	
Land use/cover	**Area (km²)**	**Area (%)**	**Area (km²)**	**Area (%)**	**Area (km²)**	**Area (%)**	**Area (km²)**	**Area (%)**
Forest land	1071.00	29.15	1523.96	41.48	1143.45	31.12	736.31	20.04
Grass land	2180.00	59.34	642.35	17.48	682.09	18.57	99.80	2.72
Crop land	315.86	8.60	1475.47	40.16	1837.63	50.02	2822.27	76.82
Water bodies	0.04	0.00	31.01	0.84	0.68	0.02	0.38	0.01
Settlement	0.22	0.01	0.31	0.01	8.33	0.23	13.67	0.37
Bare land	106.89	2.91	0.91	0.02	1.84	0.05	1.57	0.04
Total	**3674.01**	**100.00**	**3674.01**	**100.00**	**3674.01**	**100.00**	**3674.01**	**100.00**

forest cutting and facilitated plantation and growth of trees and vegetation.

Before 1984, the Rwandese and Congolese refugees who had migrated to western Uganda due to wars had opened the area in demand for land for farming reducing the forest cover. These were later resettled to other areas in the refugee camps of settlement, leaving the vegetation to recover in 1984–1999, in addition to the good government policy. The reduction in the grassland and forest land between 2000 and 2014 could be a result of ever-increasing agricultural land due to the increasing population and settlement within the area.

Waterbody area coverage reduced by 2014 and the reduction in the area is attributed to the inadequate less-monitored policy by the National Environmental Authority (NEMA) resulting in severe encroachment in the farm area.

Land-use validation and projection

Table 9 shows final Kappa statistics and percentage correctness of simulated land use of 2014 in reproducing reference/classified 2014 land cover during model validation. 77.1% correctness and overall Kappa value of 0.594 estimated by MOLUSCE indicate good ability of the model in projecting future land-use/cover of the catchment. The simulated 2014 land use depended on the transition matrix (Table 10) between 1984 and 2000 land-use/cover.

Based on the validated model, 2060 land-use/cover of Muzizi catchment (Figure 2(d)) projected using the transition matrix between 1984–2000 (Table 10) and 2000–2014 (Table 11) shows a considerable increase in cropland area and settlement area to 76.82 and 0.37%, respectively, as compared to their respective values in 2014. Forest land, grassland, and bare land all reduce from 31.12 to 20.04%, 18.57 to 2.17%, and 0.05 to 0.04%, respectively, as compared to their respective previous 2014 land-use/cover.

Table 9 | Accuracy assessment of simulated 2014 LULC in reproducing reference 2014 LULC

% Correctness	Kappa (overall)	Kappa (heist)	Kappa (loc)
77.10322	0.59356	0.5943	0.99876

Muzizi catchment current water resources and hydropower reliability

Observed flow

The daily flows at Muzizi vary from 0.88 to 85.52 m³/s, with an average value of 11.05 m³/s. The monthly flow at the project site varies from 0.99 to 47.7 m³/s. The average of mean monthly flows at the site varies from 4.7 m³/s in February to 28.41 m³/s in November as shown in Table 12. The mean annual flow at the site, excluding the years with missing data, varies from a minimum of 5.79 m³/s to a maximum of 14.65 m³/s. The mean annual flow is 11.14 m³/s.

Table 10 | Transition matrix between 1984 and 2000 land use used in simulating 2014 land use

Transition matrix 1984–2000

Land use	Forest	Grass land	Cropland	Water bodies	Settlement	Bare land
Forest	0.732148	0.056661	0.206538	0.004635	0.000003	0.000016
Grass	0.304993	0.218112	0.467041	0.009701	0.000064	0.000088
Crop land	0.182831	0.249257	0.549756	0.017408	0.000198	0.000550
Water bodies	0.000000	0.000000	1.000000	0.000000	0.000000	0.000000
Settlement	0.025000	0.475000	0.000000	0.500000	0.000000	0.000000
Bare land	0.155318	0.300829	0.536605	0.002928	0.000965	0.003354

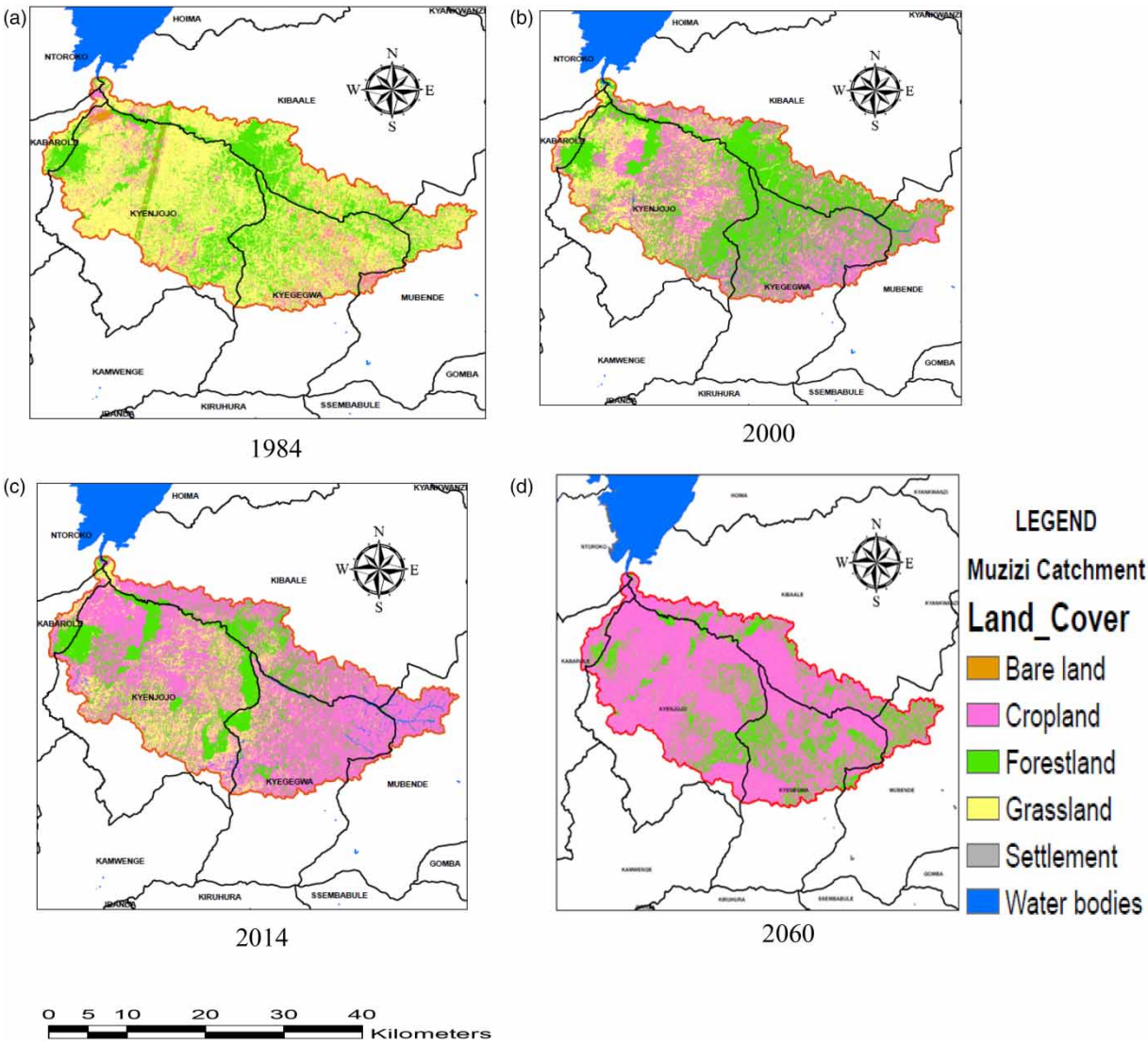

Figure 2 | Land-use/cover map for Muzizi River catchment for the years (a) 1984, (b) 2000, (c) 2014, and (d) the projected land use for the midcentury 2060.

Table 11 | Transition matrix between 2000 and 2014 land use in simulating 2060 land use

Transition matrix 2000–2014

Land use	Forest	Grass land	Cropland	Water bodies	Settlement	Bare land
Forest	0.503165	0.174744	0.321549	0.000142	0.000389	0.000012
Grass	0.083240	0.214462	0.700141	0.000167	0.000711	0.001279
Crop land	0.207606	0.201135	0.589441	0.000113	0.000950	0.000755
Water bodies	0.323939	0.283398	0.389594	0.003069	0.000000	0.000000
Settlement	0.000000	0.280802	0.719198	0.000000	0.000000	0.000000
Bare land	0.104953	0.107311	0.746462	0.000000	0.000000	0.041274

Table 12 | Monthly and annual flow series and their statistics for Muzizi site

Year	Jan	Feb	March	April	May	June	July	Aug	Sep	Oct	Nov	Dec	Annual
1998			6.37	7.20	7.66	5.69	4.08	4.18	4.11	9.29	17.07	5.08	
1999	3.96	2.98	3.33	4.49	3.85	2.29	1.22	3.27	7.07	12.41	30.38	34.92	9.18
2000	6.50	2.90	1.90	4.19	4.08	2.47	2.03	5.47					
2001	5.54	2.40	1.89	5.30	10.63	6.40	4.01	6.52	9.74	24.45	38.62	28.74	12.02
2002	9.74	2.55	2.49	5.71	32.04	8.60	2.78	4.97	6.02	10.67	33.53	28.00	12.26
2003	16.92	5.57	4.14	4.55	15.59	16.10	11.50	7.21	15.64	19.64	31.07	27.92	14.65
2004	11.99	7.54	3.68	6.43	14.64	8.51	2.75	4.27	4.38	9.44	36.87	23.51	11.14
2005	6.59	2.65	2.98	4.68	12.02	15.32	8.41	4.82	19.57	27.20	38.32	21.68	13.69
2006	9.85	5.32	4.33	18.44	19.59	11.30	4.84	4.12	4.81	18.12	28.61		
2007	28.38	14.23	12.37	11.74	11.46	21.14	22.16	31.94	38.16	47.71		30.96	
2008	13.18	6.76	4.15	12.05	8.77	4.84	1.98	3.11	8.06	18.72	28.74	9.60	10.00
2009	1.88	2.73	2.90	1.73	1.70	2.56	1.62	0.99	3.32	12.25	16.17	21.66	5.79
2010	12.51	2.52	16.98	14.25	23.80	13.15	5.55	4.83	4.80	11.13	22.48	12.58	12.05
2011	5.65	2.82	4.08	5.01	7.08	5.55	4.84	7.54	23.86	24.57	23.27	13.27	10.63
2012	4.96												
Statistic													
Mean	9.83	4.69	5.11	7.55	12.55	8.85	5.56	6.66	10.66	16.83	28.41	21.26	11.14
Minimum	1.88	2.40	1.89	1.73	1.70	2.29	1.22	0.99	3.32	9.29	16.17	5.08	5.79
Maximum	28.38	14.23	16.98	18.44	32.04	21.14	22.16	31.94	38.16	47.71	38.62	34.92	14.65

Current water availability for hydropower

The analysis of daily flow data duration for the period of 1998–2012 is presented in Figure 3 after the subtraction of environmental flow (0.69 m^3/s), which is termed as flow available for hydropower production. Available flow exceeded 95% of the time was termed as firm flow (read from FDC after the subtraction of environmental flow) is estimated as 0.92 m^3/s.

SWAT modelling

SWAT calibration and validation

The semi-distributed SWAT hydrologic model was calibrated and validated for Muzizi streamflow gauges. As shown in Figure 4(a) and 4(b), respectively, the model was able to simulate daily streamflows with the goodness-of-fit values of NSE 64.5%, PBIAS 4.5, and R^2 0.59 for the calibration period

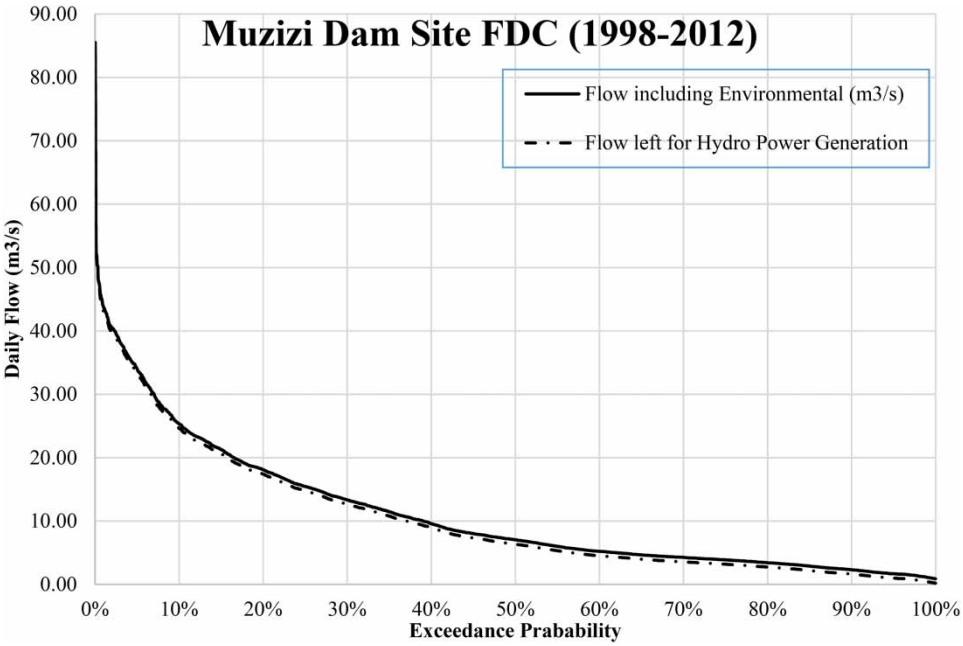

Figure 3 | Muzizi River flow duration curve – 1998–2012.

(2002–2007) and NSE 56.3%, PBIAS −18.3, and R^2 0.51 for the validation periods (2008–2010). Simulated and observed discharge values during validation (2008–2010) show a fairly good match with NSE and PBIAS and R^2. However, the observed peak flows during calibration and validation were not well captured by the model.

Sensitivity analysis

The SWAT-CUP was applied to perform a global sensitivity analysis of 14 flow parameters used for the calibration of the SWAT model. The results showed that out of the 16 flow parameters, only nine were very sensitive to flow. The rankings of the flow parameters are presented in Appendix 2, while the fitted values for the most sensitive parameters are indicated in Appendix 3. The most sensitive parameter was the SCS runoff curve number (CN2). The curve number estimates runoff based on the relationship between precipitation, hydrologic soil group, and land uses. Other researchers (Mutenyo *et al.* 2011; Zuo *et al.* 2016) have also found the SCS curve number to be the most sensitive streamflow parameter in modeling hydrology in their studies. The other sensitive parameters included the V__ALPHA_BF.gw, V__HRU_SLP.hru, R__SOL_K(..).sol, V__REVAPMN.gw, V__EPCO.bsn, V__LAT_TTIME.hru, V__GW_REVAP.gw, and V__SOL_AWC (..).sol.

Climate model performance

Precipitation

The daily precipitation simulations of the climate models from the CORDEX-Africa RCM datasets were averaged over the basin area, and their performances were evaluated using statistical parameters. The mean monthly, mean daily, and mean annual precipitation for the historical period 1981–2005 were compared with the CHIRPS reanalysis dataset for the same period. Summary statistics used to assess GCMs' performances in simulating observed rainfall are shown in Appendix 4.

Maximum and minimum temperature

Comparison of daily average maximum/minimum temperature for the period of 1981–2005 was compared to that of CFSR reanalysis over the catchment for the same period. The null hypothesis was not rejected for all models as evident by their respective *p*-values being less than 5%. The RACMO22T model was selected as the best model in simulating the observed maximum/minimum temperature over the catchment. This is due to its high values of R^2, NSE, and *R*s and very low values of PBIAS and RMSE as shown in Appendix 5. On the other hand, REMO and

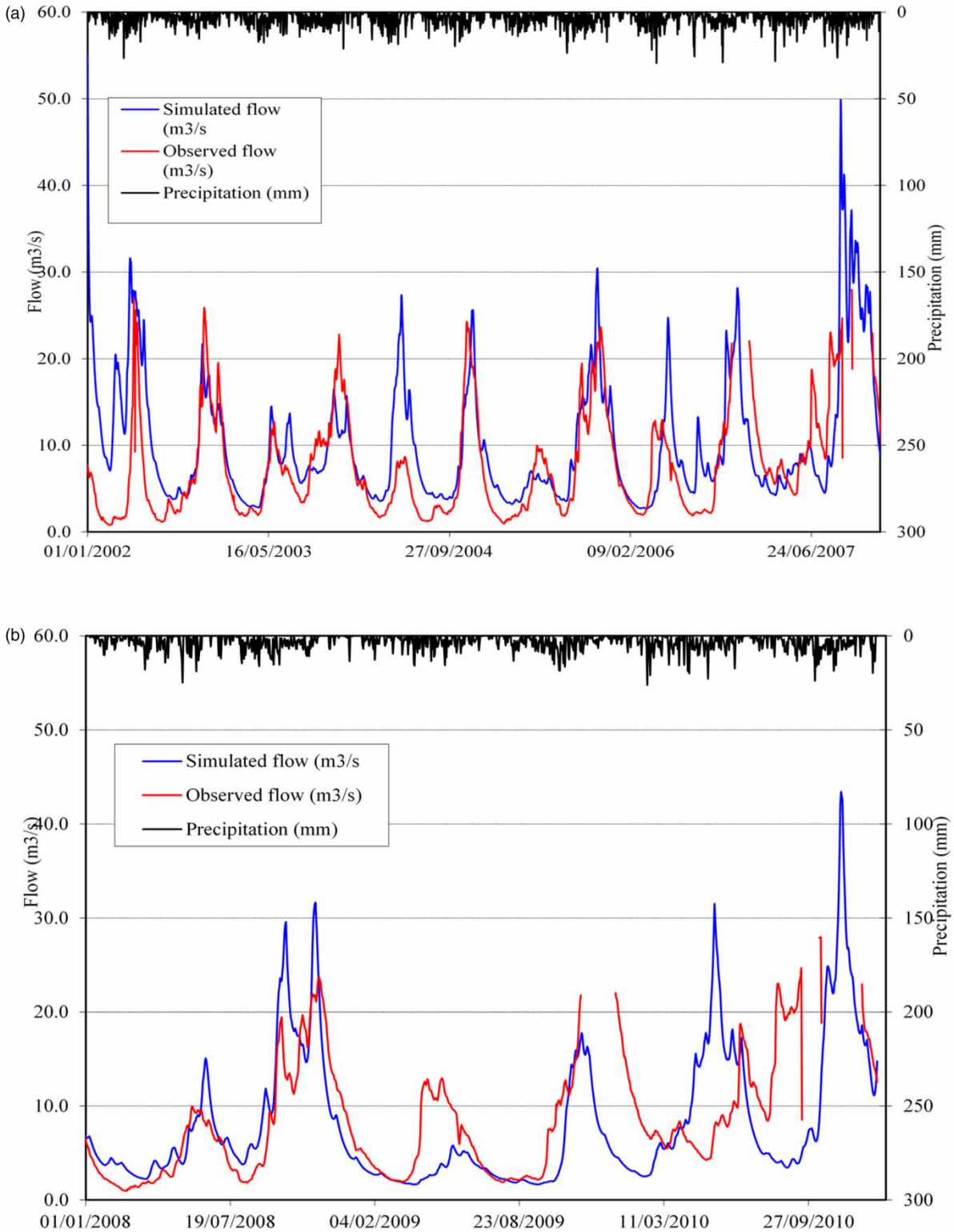

Figure 4 | (a) Simulated versus observed streamflow of Muzizi River for the calibration periods (2002–2007) at Gauge Station 85211. (b) Simulated versus observed streamflow of Muzizi River for the validation periods (2008–2010) at Gauge Station 85211.

RCA4 RCM performed best in reproducing mean monthly, daily, and annual precipitation.

Potential change in mean monthly and annual precipitation

Future/midcentury rainfall has been differentiated at the scale of the catchment when possible (depending on the resolution used for the different climate modeling). Table 13 shows the evolution of mean monthly rainfall for the different scenarios (for the time 2041–2060 from the reference/historical period of 1981–2005) for the Muzizi basin.

The different scenarios indicate little change (increase) in annual total in the percentage range of 2–10% for all the scenarios (including an average of all scenarios). Rainfall distribution during the year is likely to change with the period from July to October likely to be dryer than it used to be, whereas January to June and November to December will tend to be wetter. Mean monthly precipitation for the average of REMO and RCA4 under RCP4.5 is expected to increase for January–July (with the percentage change in the range of 5–20%) and November–December (31–34%) with an annual change of 5%. For the case of the RCP8.5 scenario, the average of REMO and RCA4 mean monthly precipitation will increase for January, February, April, June, November, and December.

Potential change in mean monthly and annual maximum and minimum temperatures

Tables 14 and 15 show the evolution of mean monthly and average annual minimum and maximum temperatures for the different scenarios (for time 2041–2060 from the reference/historical period of 1981–2005) for the Muzizi basin, respectively.

The different scenarios indicate little increase in an annual minimum temperature in the range of 0.8–2.5% and an annual maximum temperature in the range of 0–0.4% for all the scenarios (including an average of all scenarios) for both REMO and RCA4 RCM. Mean monthly minimum temperature under average of REMO and RCA4 RCM for RCP 4.5 is predicted to increase for January to July (in the range of 2.0–4.4%) and September to December (in the range of 0.4–2.1%) while for RCP 8.5 it will increase in the same month range but with minimum temperature in the range of 1.1–3.8% and 1.1–2.8%, respectively, for the same month range. The mean monthly minimum temperature is predicted to decrease for August for all the scenarios for both REMO and RCA4 RCM. Both REMO and RCA4 RCM under RCP4.5 and RCP8.5 scenarios projected a decline in mean monthly maximum temperature for February, April to June, and September to October.

Table 13 | Midcentury mean monthly and annual rainfall under different climate change scenarios (RCP4.5 and RCP8.5)

Month	REMO–RCP4.5 (2041–2060)	REMO–RCP8.5 (2041–2060)	RCA4–RCP4.5 (2041–2060)	RCA4–RCP8.5 (2041–2060)	Average of REMO and RCA–RCP4.5 (2041–2060)	Average of REMO and RCA–RCP8.5 (2041–2060)	Average of all scenarios	Range
Jan	− 18%	53%	27%	172%	5%	113%	59%	− 18 – 172%
Feb	− 43%	− 9%	51%	96%	4%	43%	24%	− 45 – 96%
March	− 5%	− 22%	26%	7%	10%	− 7%	1%	− 5 – 26%
April	1%	15%	13%	9%	7%	12%	10%	1 – 15%
May	12%	2%	− 1%	− 8%	5%	− 3%	1%	− 3 – 12%
June	27%	20%	14%	26%	20%	23%	22%	14 – 27%
July	35%	− 63%	− 5%	6%	15%	− 29%	− 7%	− 63–35%
Aug	7%	− 30%	− 26%	− 22%	− 10%	− 26%	− 18%	− 30–7%
Sep	− 17%	− 14%	− 15%	− 18%	− 16%	− 16%	− 16%	− 18–14%
Oct	− 25%	− 14%	− 3%	− 9%	− 14%	− 12%	− 13%	− 25 to −3%
Nov	60%	76%	8%	11%	34%	43%	39%	8 – 60%
Dec	4%	8%	58%	49%	31%	28%	30%	4–58%
Annual	4%	2%	7%	10%	5%	6%	6%	2–10%

Table 14 | Midcentury mean monthly and annual minimum temperature under different climate change scenarios (RCP4.5 and RCP8.5)

Month	REMO–RCP4.5 (2041–2060)	REMO–RCP8.5 (2041–2060)	RCA4–RCP4.5 (2041–2060)	RCA4–RCP8.5 (2041–2060)	Average of REMO and RCA–RCP4.5 (2041–2060)	Average of REMO and RCA–RCP8.5 (2041–2060)	Average of all scenarios	Range
Jan	2.5%	3.1%	3.0%	4.4%	2.7%	3.8%	3.2%	2.5–4.4%
Feb	1.7%	1.8%	2.2%	3.2%	2.0%	2.5%	2.2%	1.7–3.2
March	0.9%	1.1%	1.4%	2.4%	1.1%	1.7%	1.4%	0.9–2.4%
April	0.6%	0.7%	1.1%	2.1%	0.9%	1.4%	1.1%	0.6–2.1%
May	1.5%	1.8%	2.0%	3.2%	1.7%	2.5%	2.1%	1.5–3.2%
June	0.4%	0.7%	0.9%	2.5%	0.6%	1.6%	1.1%	0.4–2.5%
July	0.0%	0.2%	0.5%	2.0%	0.3%	1.1%	0.7%	0.0–2.0%
Aug	− 3.3%	− 3.7%	− 2.8%	− 2.0%	− 3.1%	− 2.8%	− 3.0%	− 3.7–2%
Sep	1.9%	1.9%	2.4%	3.7%	2.1%	2.8%	2.5%	1.9–3.7%
Oct	0.9%	1.0%	1.4%	2.8%	1.1%	1.9%	1.5%	0.9–2.8%
Nov	0.2%	0.4%	0.7%	1.8%	0.4%	1.1%	0.8%	0.2–1.8%
Dec	2.7%	2.9%	3.2%	4.2%	3.0%	3.5%	3.2%	2.7–4.2%
Annual	0.8%	1.0%	1.3%	2.5%	1.1%	1.8%	1.4%	0.8–2.5%

Table 15 | Midcentury mean monthly and annual maximum temperature under different climate change scenarios (RCP 4.5 and RCP8.5)

Month	REMO–RCP4.5 (2041–2060)	REMO–RCP8.5 (2041–2060)	RCA4–RCP4.5 (2041–2060)	RCA4–RCP8.5 (2041–2060)	Average of REMO and RCA–RCP4.5 (2041–2060)	Average of REMO and RCA–RCP8.5 (2041–2060)	Average of all scenarios	Range
Jan	0.1%	0.4%	0.1%	0.4%	0.1%	0.4%	0.3%	0.1–0.4%
Feb	-0.3%	0.1%	− 0.3%	0.1%	− 0.3%	0.1%	− 0.1%	0.3–0.1%
March	1.0%	1.1%	1.0%	1.1%	1.0%	1.1%	1.1%	1–1.1%
April	− 0.2%	− 0.2%	− 0.2%	− 0.2%	− 0.2%	− 0.2%	− 0.2%	− 0.2%
May	− 0.2%	0.4%	− 0.2%	0.4%	− 0.2%	0.4%	0.1%	− 0.2–0.4%
June	− 1.7%	− 1.3%	− 1.7%	− 1.3%	− 1.7%	− 1.3%	− 1.5%	− 1.7–1.3%
July	0.8%	1.1%	0.8%	1.1%	0.8%	1.1%	1.0%	0.8–1.1%
Aug	2.7%	2.6%	2.7%	2.6%	2.7%	2.6%	2.7%	2.6–2.7%
Sep	− 3.0%	− 2.3%	− 3.0%	− 2.3%	− 3.0%	− 2.3%	− 2.7%	− 3–2.3%
Oct	− 1.9%	− 1.1%	− 1.9%	− 1.1%	− 1.9%	− 1.1%	− 1.5%	− 1.9–−1.1%
Nov	0.9%	1.0%	0.9%	1.0%	0.9%	1.0%	1.0%	0.9–1%
Dec	2.1%	2.8%	2.1%	2.8%	2.1%	2.8%	2.4%	2.1–2.8
Annual	0.0%	0.4%	0.0%	0.4%	0.0%	0.4%	0.2%	0–0.4%

Potential change in flow and hydropower generation of Muzizi River

Potential change in firm flow and firm power capacity of Muzizi River

Figure 5(a) and 5(b) show the potential change in firm flow (Q95) and firm power capacity of Muzizi River, while firm flow corresponding to 95% exceedance probability of Muzizi River for the reference and midcentury discharges under RCP4.5 and RCP8.5 scenarios, respectively.

The results show that the firm flow corresponding to equaled/exceeded 95% of the time is expected to rise from 0.92 to 4.48 m^3/s (387%) and 4.01 m^3/s (336%) under RCP4.5 and RCP8.5 climate change scenarios, respectively, for REMO RCM which correspond to firm hydropower

(a)

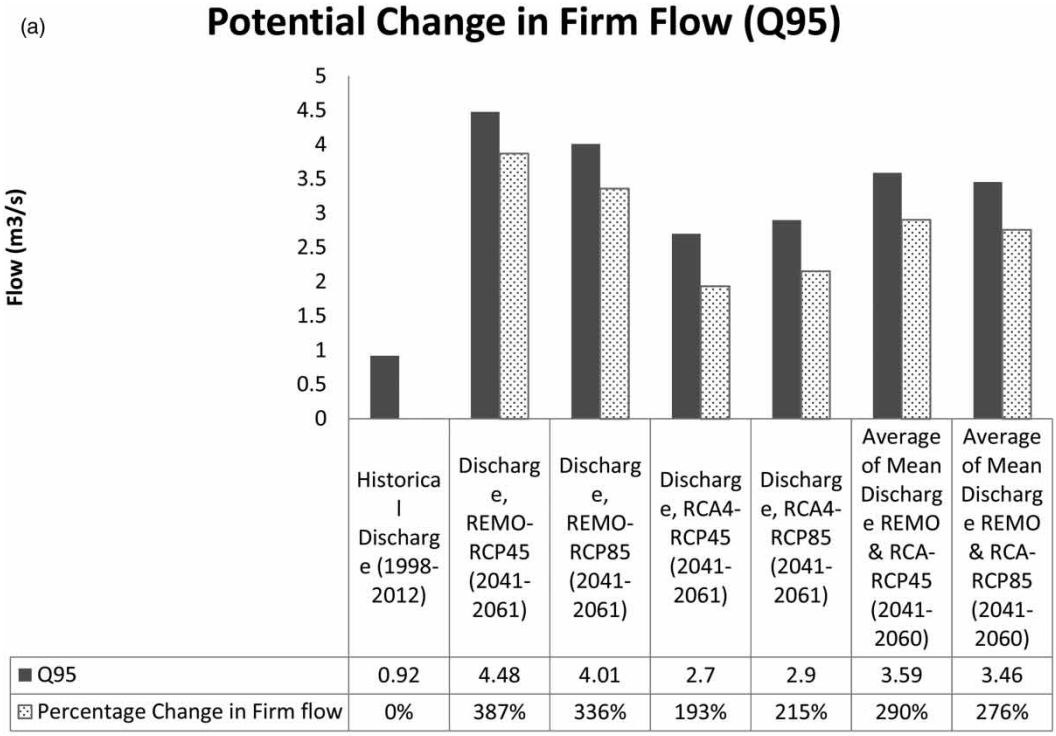

	Historical Discharge (1998-2012)	Discharge, REMO-RCP45 (2041-2061)	Discharge, REMO-RCP85 (2041-2061)	Discharge, RCA4-RCP45 (2041-2061)	Discharge, RCA4-RCP85 (2041-2061)	Average of Mean Discharge REMO & RCA-RCP45 (2041-2060)	Average of Mean Discharge REMO & RCA-RCP85 (2041-2060)
■ Q95	0.92	4.48	4.01	2.7	2.9	3.59	3.46
⊡ Percentage Change in Firm flow	0%	387%	336%	193%	215%	290%	276%

(b)

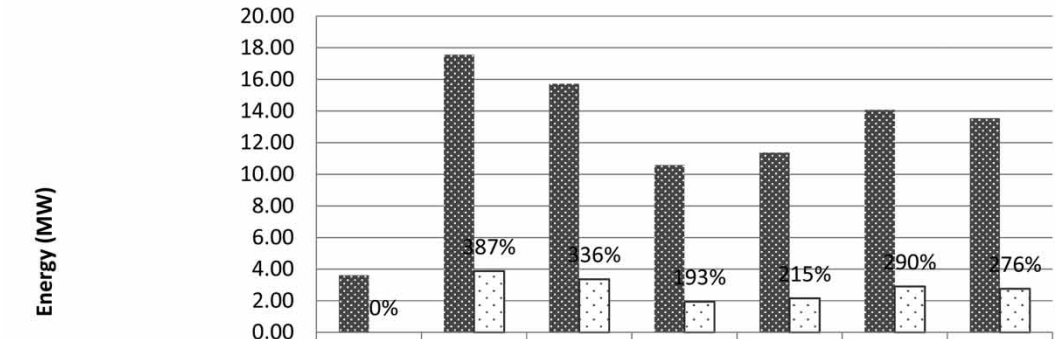

	Historical Firm Power Capacity (1998-2012)	Firm Power capacity, REMO-RCP45 (2041-2061)	Firm Power capacity, REMO-RCP85 (2041-2061)	Firm Power capacity, RCA4-RCP45 (2041-2061)	Firm Power capacity, RCA4-RCP85 (2041-2061)	Average of Firm Power capacity REMO & RCA-RCP45 (2041-2060)	Average of Firm Power capacity REMO & RCA-RCP85 (2041-2060)
▩ Power Capacity	3.61	17.56	15.72	10.59	11.37	14.07	13.55
☐ Percentage Change in Power capacity	0%	387%	336%	193%	215%	290%	276%

Figure 5 | (a) Comparison of current and midcentury firm flow for Muzizi River under different climate change scenarios. (b) Comparison of current and midcentury firm power capacity for Muzizi River under different climate change scenarios.

generation/production capacity of 17.56 and 15.72 MW under the two scenarios, respectively, from the reference 3.61 MW. From reference firm discharge of 0.92 m^3/s, RCA4 RCM projected firm flow to 2.7 m^3/s (193%) and 2.9 m^3/s (215%) under RCP4.5 and RCP8.5 scenarios, respectively, corresponding to the projected future firm discharge of 10.59 and 11.37 MW. The average of REMO and RCA4 projected firm flow to 3.59 and 3.46 m^3/s, which corresponds to the future firm power capacity of 14.07 and 13.55 MW under RCP4.5 and RCP8.5, respectively.

The results show that the firm flow corresponding to equaled/exceeded 95% of the time is expected to rise from 0.92 to 4.48 m^3/s (387%) and 4.01 m^3/s (336%) under RCP4.5 and RCP8.5 climate change scenarios, respectively, for REMO RCM which correspond to firm hydropower generation/production capacity of 17.56 and 15.72 MW under the two scenarios, respectively, from the reference 3.61 MW. From the reference firm discharge of 0.92 m^3/s, RCA4 RCM projected firm flow to 2.7 m^3/s (193%) and 2.9 m^3/s (215%) under RCP4.5 and RCP8.5 scenarios, respectively, corresponding to the projected future firm discharge of 10.59 and 11.37 MW. The average of REMO and RCA4 projected firm flow to 3.59 and 3.46 m^3/s which corresponds to the future firm power capacity of 14.07 and 13.55 MW under RCP4.5 and RCP8.5, respectively.

Potential change in mean daily flow and mean power generation of Muzizi River

Figure 6(a) and 6(b) compare the reference mean daily flow of Muzizi River with midcentury mean daily flow under RCP4.5 and RCP8.5 climate change scenarios for both REMO and RCA4 RCM, respectively. The average daily flow for REMO and RCA4 RCM is expected to rise to 24.1 and 20.0 m^3/s, respectively, under the RCP4.5 climate change scenario which is equivalent to a percentage change of 118 and 81%, respectively. This, however, corresponds to the expected midcentury hydropower generation capacity of 94.47 MW. Under the RCP8.5 scenario, both REMO and RCA4 RCM projected average daily flow/hydropower capacity to 20.7 m^3/s (corresponding to 81.06 MW) and 22.8 m^3/s (corresponding to 89.4 MW), respectively, as compared to historical 11.05 m^3/s average daily flow with 43.32 MW estimated in this study. The average of REMO and RCA4 mean daily discharge is expected to rise by 100 and 97% to 22.0 and 21.7 m^3/s under RCP4.5 and RCP8.5 climate change scenarios when compared with an estimated mean daily discharge in this study. Energy generated under RCP4.5 and RCP8.5 for an average of REMO and RCA4 RCM is expected to rise to 86.4 and 85.2 MW, respectively.

Potential change in minimum, maximum, and mean annual flow

About historical/current minimum, maximum, and mean annual flow of Muzizi River, future minimum, maximum, and mean annual flow will increase to 11.25, 38.25, and 23.91 m^3/s of average REMO and RCA4 RCM mean annual flow, respectively, under RCP4.5, while under the RCP8.5 scenario, an average of REMO and RCA4 RCM for maximum and mean annual flow is projected to rise to 34.33 and 26.55 m^3/s, respectively, but the minimum mean annual flow will drop to 5.01 m^3/s.

Potential change in Muzizi River mean monthly flow

As presented in Table 16, the average of REMO and RCA4 mean monthly flow under RCP4.5 is expected to rise considerably for all of the months in the range of 8–224%; however, these values are expected to rise higher under the RCP8.5 climate change scenario for all the months, except for September and October where the mean annual flow is expected to be lower as compared with the historical one.

Potential change in mean monthly and annual energy generation

Figure 7 shows that there is an increase in hydropower generation in the wet season of March to May (MAM), except for the wet season of September to November (SON) where mean monthly hydropower generation for REMO (under RCP8.5) and RCA4 RCM (under RCP4.5) is expected to decrease to 28.49 and 41.31 MW, respectively, for different scenarios particularly for September, as compared with the reference period. Hydropower generated by the

(a)

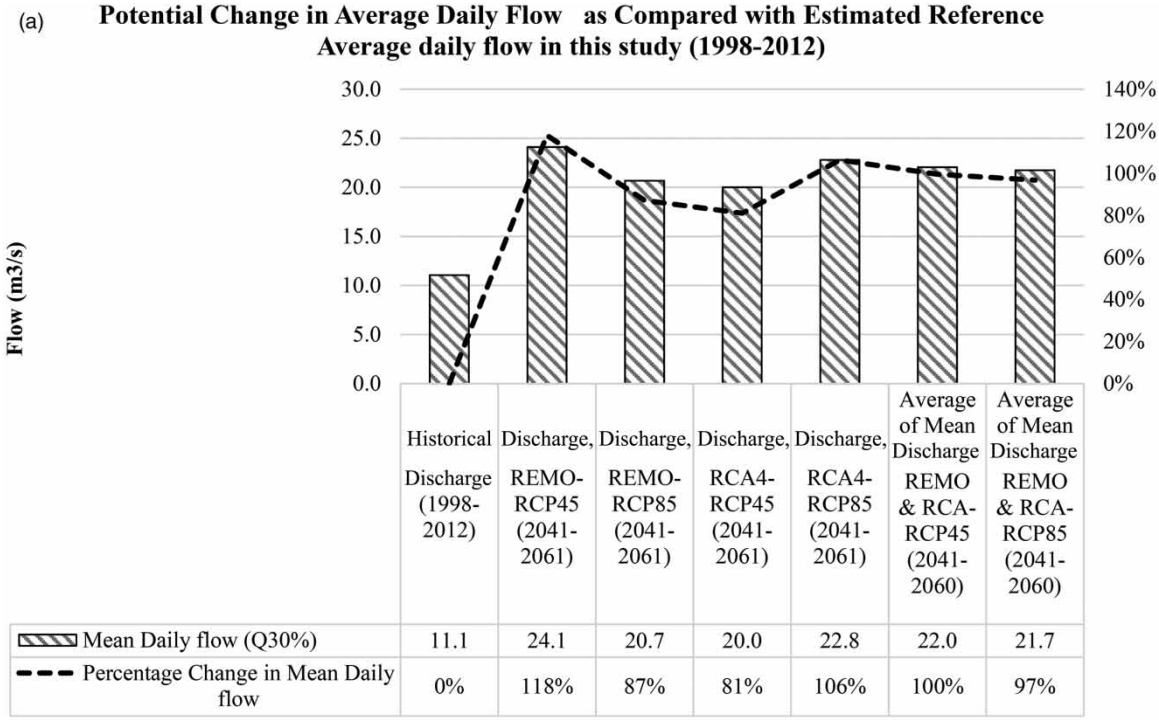

	Historical Discharge (1998-2012)	Discharge, REMO-RCP45 (2041-2061)	Discharge, REMO-RCP85 (2041-2061)	Discharge, RCA4-RCP45 (2041-2061)	Discharge, RCA4-RCP85 (2041-2061)	Average of Mean Discharge REMO & RCA-RCP45 (2041-2060)	Average of Mean Discharge REMO & RCA-RCP85 (2041-2060)
Mean Daily flow (Q30%)	11.1	24.1	20.7	20.0	22.8	22.0	21.7
Percentage Change in Mean Daily flow	0%	118%	87%	81%	106%	100%	97%

(b)

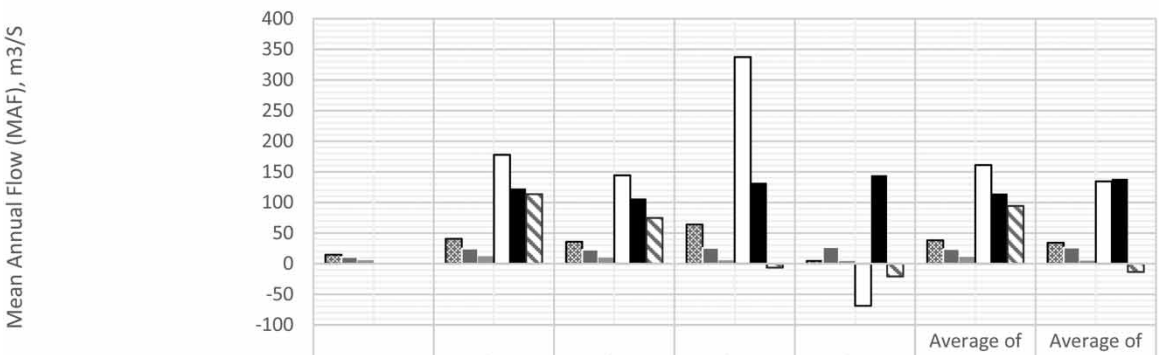

	Historical Discharge (1998-2012)	Discharge, REMO-RCP45 (2041-2061)	Discharge, REMO-RCP85 (2041-2061)	Discharge, RCA4-RCP45 (2041-2061)	Discharge, RCA4-RCP85 (2041-2061)	Average of Mean Discharge REMO & RCA-RCP45 (2041-2060)	Average of Mean Discharge REMO & RCA-RCP85 (2041-2060)
Max MAF	14.65	40.70	35.79	64.08	4.59	38.25	34.33
MAF	11.14	24.81	23.00	25.88	27.22	23.91	26.55
Min MAF	5.79	12.37	10.13	5.43	4.59	11.25	5.01
Percentage Change in Max MAF	0	178	144	337	-69	161	134
Percentage Change in MAF	0	123	106	132	144	115	138
Percentage Change in Min MAF	0	114	75	-6	-21	94	-14

Figure 6 | (a) Potential change in mean daily flow (2041–2060) as compared with estimated reference (1998–2012) average daily flow in this study. (b) Potential change in mean annual flow.

Table 16 | Midcentury mean monthly flow under different climate change scenarios (RCP4.5 and RCP8.5)

Month	REMO–RCP4.5 (2041–2060)	REMO–RCP8.5 (2041–2060)	RCA4–RCP4.5 (2041–2060)	RCA4–RCP8.5 (2041–2060)	Average of REMO and RCA–RCP4.5 (2041–2060)	Average of REMO and RCA–RCP8.5 (2041–2060)
Jan	102%	152%	205%	259%	153%	206%
Feb	82%	175%	223%	621%	152%	398%
March	22%	60%	280%	440%	151%	250%
April	86%	137%	363%	393%	224%	265%
May	157%	204%	179%	169%	168%	187%
June	190%	191%	166%	178%	178%	185%
July	182%	118%	190%	154%	186%	136%
Aug	173%	−1%	67%	66%	120%	33%
Sep	103%	−32%	−1%	25%	51%	−4%
Oct	38%	−24%	−22%	−7%	8%	−16%
Nov	111%	93%	18%	22%	65%	57%
Dec	178%	191%	251%	146%	215%	168%

average of both REMO and RCA4 RCM under the RCP8.5 scenario will be lower than the reference power for September (40.29 MW) and October (55.53 MW). The months of December to February (DJF) and June to July (JJA) considered as dry months for the region are projected to have a considerable increase in hydropower generation for all the scenarios. Power generation under the average of REMO and RCA4 RCM discharge for both scenarios for all the months is projected to be higher than the reference power generation.

Mean annual hydropower output is presented in Table 17 and is expected to rise significantly from the current 386.27 GW h (as estimated in this study) to 867.82 and 862.52 GW h under RCP4.5 and RCP8.5 climate change scenarios, respectively, for an average of REMO and RCA4 RCM under consequences of a 125 and 123% (76% 24b) (Table 17) increase in mean annual streamflow under an assumption of 0.01 and 0.12 °C increase in mean annual maximum temperature, and 0.17 and 0.28 °C increase in mean annual minimum temperature and 5 and 6% increase in mean annual rainfall under RCP4.5 and RCP8.5 climate change scenarios for an average of REMO and RCA4 RCM.

CONCLUSION AND RECOMMENDATIONS

Conclusions

This study has shown that it is possible to utilize bias-corrected reanalysis data and historical discharge data to build a climate model in a data-scarce scenario as well as evaluate the potential impacts of land use and climate change on the hydropower reliability of rivers such as Muzizi River. CHIRPS reanalysis rainfall after performance evaluation with observed rainfall was bias corrected using the Delta change correction method and selected as one of the hydro-meteorological inputs together with accuracy assessed 2014 land use for SWAT model simulation run during calibration (2002–2007) and validation periods (2008–2010).

The statistical analysis produced NSE and R^2 of 64.5% and 0.59, respectively, for the calibration period and 56.3 and 0.51%, respectively, for the validation period which were considered acceptable. Six LULC scenarios (deforestation, 31–20%; grassland, 19–3%; cropland, 50–77%; water bodies, 0.02–0.01%; settlement, 0.23–0.37%, and barren land 0.055–0.046% for projected 2060 land use from the reference land use of 2014) and three downscaled RCM (REMO and RCA4 for precipitation and RACMO22T for temperature from a pool of four CORDEX-Africa RCMs) were examined. A calibrated/validated SWAT simulation model was applied for the midcentury (2041–2060) period, and potential change in hydropower energy about mean daily flow (design/optimum flow $\geq$ 30% exceedance probability) and firm flow (flow $\geq$ 95% exceedance probability) and mean annual energy were evaluated under the condition of altered runoff under RCP4.5 and RCP8.5 climate change scenarios. There will be a significant increase in midcentury firm hydropower capacity from 3.61 to 14.05 MW and 13.55 MW under RCP4.5 and RCP8.5 climate change scenarios, respectively, for an average of REMO and RACMO22T RCM. The study further reveals that if land use and climate change impacts were considered in estimating mean daily (optimum/design) flow, then optimum hydropower capacity under RCP4.5 and RCP8.5 climate change scenarios (for an average of REMO and RCA4 RCM) should have been 86.44 and 85.23 MW, respectively, compared to the currently estimated 46.9 MW

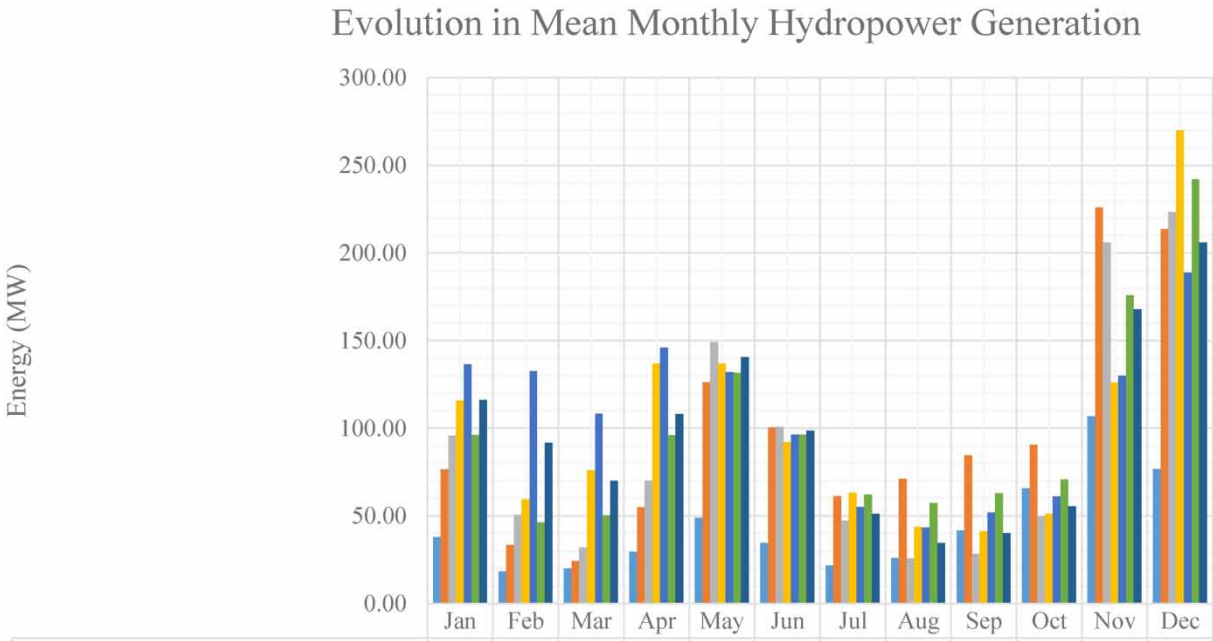

	Jan	Feb	Mar	Apr	May	Jun	Jul	Aug	Sep	Oct	Nov	Dec
Reference Energy genration (1998-2012)	38.04	18.42	20.05	29.62	49.10	34.70	21.79	26.11	41.78	65.83	106.91	76.79
Mean monthy Energy, REMO-RCP45 (2041-2060)	76.70	33.46	24.46	55.01	126.40	100.51	61.35	71.31	84.65	90.67	225.95	213.78
Mean monthy Energy , REMO-RCP85 (2041-2060)	95.88	50.63	31.99	70.17	149.30	101.03	47.39	25.80	28.49	49.83	206.10	223.22
Mean monthy Energy, RCA4-RCP45 (2041-2060)	115.93	59.45	76.18	137.01	136.98	92.25	63.20	43.72	41.31	51.27	126.17	269.85
Mean monthy Energy, RCA4-RCP85 (2041-2060)	136.52	132.77	108.32	146.13	132.04	96.52	55.26	43.47	52.08	61.23	130.01	188.87
Mean monthy Energy REMO & RCA-RCP45 (2041-2060)	96.32	46.45	50.32	96.01	131.69	96.38	62.27	57.52	62.98	70.97	176.06	241.82
Mean monthy Energy REMO & RCA-RCP85 (2041-2060)	116.20	91.70	70.15	108.15	140.67	98.77	51.33	34.64	40.29	55.53	168.06	206.05

Figure 7 | Comparison of predicted average monthly hydropower generation in assumed climate change scenarios with that in the reference scenario.

Table 17 | Predicted mean annual hydropower generation for different scenarios and their deviations from mean annual hydropower output estimated in this study

Scenario	Average annual hydropower generation (GW h)	Increment of annual hydropower generation (%)	Average annual hydropower generation in dry season (GW h)	Change in annual hydropower generation in dry season (%)
Reference	386.27	0	241.20	0
Mean annual Energy-REMO and RCA4–RCP4.5 (2041–2060)	867.82	125	631.22	162
Mean annual Energy-REMO and RCA4–RCP8.5 (2041–2060)	862.52	123	539.42	124

by UEGCL. Mean annual hydropower capacity is expected to rise significantly from the current 386.27 GW h (as per estimate in this study) and 488.1 GW h UEGCL to 867.82 GW h and 862.52 GW h under RCP4.5 and RCP8.5 climate change scenarios, respectively, for an average of REMO and RCA4 RCM under consequences of a 125 and 123% increase in mean annual streamflow under an assumption of 0.01 and 0.12 °C increase in mean annual maximum temperature and 0.17 and 0.28 °C increase in mean annual minimum temperature and 5 and 6% increase in mean annual rainfall under RCP4.5 and RCP8.5 climate change scenarios, respectively, for an average of REMO and RCA4 RCM. Overall, the current hydropower capacity (i.e., firm capacity and optimum/design capacity) of Muzizi HPP will still be reliable for the coming midcentury period as evidenced by the rising firm flow and design flow under the impact of land use and climate change.

Recommendations

The study aimed at contributing knowledge to the hydropower and engineering professionals on the risks of land use and climate change on the hydropower reliability in the development of hydropower plants on small, medium, and large rivers. While this has been demonstrated, it should be noted that the analysis is limited to the hydrological dimension and has not considered aspects such as sedimentation. Given that the predicted changes are due to changes in flows caused by land use and climate changes, the risk of sedimentation on hydropower plants such as this one cannot be ruled out. It is therefore recommended that authorities pursue an environmental protection agenda through reafforestation and enforcing buffer zones alongside the Muzizi River, and a policy that governs the operation of these actions on catchments is most befitting. This study did not take into consideration of sedimentation impacts on the dam and its components, and it is therefore inferred that future studies be carried out to establish this.

This study has been undertaken under limited data in terms of period and spatial distribution. While this study has demonstrated that it is possible to utilize bias-corrected reanalysis data and historical discharge data to build a climate model in a data-scarce scenario, to improve the accuracy of the results, there is a need to invest in hydrological and climate infrastructure for improved data collection. These investments can be recouped through savings from improved operation and maintenance of the hydropower plant system and reduced unplanned downtime due to hydrological catastrophes.

It has been noted that the future discharges will be more than the designed discharges creating operation and maintenance challenges. To mitigate this impact, the spillway should be re-optimized to accommodate future overflows. It is further recommended that further studies are undertaken on how to utilize this increased flow and how to optimize the performance of the plant. It has been found that climate change and land use impact river systems differently for different areas, and therefore, it is recommended that such studies are carried out on different river catchments to understand their responsibilities in the upcoming climate and land-use changes.

DECLARATION OF COMPETING INTEREST

The authors declare no conflict of interest.

ACKNOWLEDGEMENTS

The authors would like to acknowledge the moral and financial support from Water and Society (WaSo) of Makerere University. We would like to thank the reviewers for their valuable comments and suggestions in improving this manuscript.

DATA AVAILABILITY STATEMENT

All relevant data are included in the paper or its Supplementary Information.

REFERENCES

Abbaspour, K. C., Yang, J., Maximov, I., Siber, R., Bogner, K., Mieleitner, J., Zobrist, J. & Srinivasan, R. 2007 Modelling

hydrology and water quality in the pre-alpine/alpine Thur watershed using SWAT. *Journal of Hydrology* **333** (2–4), 413–430. https://doi.org/10.1016/j.jhydrol.2006.09.014.

Abbaspour, K. C., Rouholahnejad, E., Vaghefi, S., Srinivasan, R., Yang, H. & Kløve, B. 2015 A continental-scale hydrology and water quality model for Europe: calibration and uncertainty of a high-resolution large-scale SWAT model. *Journal of Hydrology* **524**, 733–752. https://doi.org/10.1016/j.jhydrol.2015.03.027.

Al-Safi, H. I. J. & Sarukkalige, P. R. 2017 Assessment of future climate change impacts on hydrological behavior of Richmond River Catchment. *Water Science and Engineering* **10** (3), 197–208. https://doi.org/10.1016/j.wse.2017.05.004.

Anaba, L. A., Banadda, N., Kiggundu, N., Wanyama, J., Engel, B. & Moriasi, D. 2017 Application of SWAT to assess the effects of land use change in the Murchison Bay Catchment in Uganda. *Computational Water, Energy, and Environmental Engineering* **06** (01), 24–40. https://doi.org/10.4236/cweee.2017.61003.

Anderson, J., Ernest, H., John, R. & Richard, W. 1976 *A Land Use and Land Cover Classification System for Use with Remote Sensor Data*. https://pubs.usgs.gov/pp/0964/report.pdf.

Arnold, J. G., Moriasi, D. N., Gassman, P. W., Abbaspour, K. C., White, M. J., Srinivasan, R., Santhi, C., Harmel, R. D., Van Griensven, A., Van Liew, M. W., Kannan, N. & Jha, M. K. 2012 SWAT: model use, calibration, and validation. *Transactions of the ASABE* **55** (4), 1491–1508. https://doi.org/10.13031/2013.42259.

Ashraf Vaghefi, S., Abbaspour, N., Kamali, B. & Abbaspour, K. C. 2017 A toolkit for climate change analysis and pattern recognition for extreme weather conditions – case study: California-Baja California Peninsula. *Environmental Modelling and Software* **96**, 181–198. https://doi.org/10.1016/j.envsoft.2017.06.033.

Atkinson, H. D. E., Johal, P., Falworth, M. S., Ranawat, V. S., Dala-Ali, B. & Martin, D. K. 2010 Adductor tenotomy: its role in the management of sports-related chronic groin pain. *Archives of Orthopaedic and Trauma Surgery* **130** (8), 965–970. https://doi.org/10.1007/s00402-009-1032-4.

Banze, F., Guo, J. & Xiaotao, S. 2018 Variability and trends of rainfall, precipitation and discharges over zambezi river basin, southern africa: review. *International Journal of Hydrology* **2** (2), 132–135. https://doi.org/10.15406/ijh.2018.02.00062.

Bayar, Y. & Özel, H. 2014 Electricity consumption and economic growth in emerging economies. *Journal of Knowledge Management, Economics and Information Technology* **4**, 15–15.

Berhanu, B., Seleshi, Y., Demisse, S. S. & Melesse, A. M. 2016 Bias correction and characterization of climate forecast system re-analysis daily precipitation in Ethiopia using fuzzy overlay. *Meteorological Applications* **23** (2), 230–243. https://doi.org/10.1002/met.1549.

Betrie, G. D., Mohamed, Y. A., Van Griensven, A. & Srinivasan, R. 2011 Sediment management modelling in the Blue Nile Basin using SWAT model. *Hydrology and Earth System Sciences* **15** (3), 807–818. https://doi.org/10.5194/hess-15-807-2011.

Bosmans, J. H. C., Beek, L. P. H. R. V., Sutanudjaja, E. H. & Bierkens, M. F. P. 2016 *Hydrological Impacts of Global Land Cover Change and Human Water use*. December, 1–31. https://doi.org/10.5194/hess-2016-621.

Cole, M. A., Elliott, R. J. R. & Strobl, E. 2014 Climate change, hydro-dependency, and the African Dam Boom. *World Development* **60**, 84–98. https://doi.org/10.1016/j.worlddev.2014.03.016.

Conway, D., Hamandawana, H., Dieulin, C. & Mahe, G. 2017 *Rainfall and River Flow Variability in Sub-Saharan Africa During the Twentieth Century Rainfall and Water Resources Variability in Sub-Saharan Africa During the Twentieth Century*. February 2017. https://doi.org/10.1175/2008JHM1004.1.

Darand, M., Amanollahi, J. & Zandkarimi, S. 2017 Evaluation of the performance of TRMM multi-satellite precipitation analysis (TMPA) estimation over Iran. *Atmospheric Research* **190**, 121–127.

Engel, B., Storm, D., White, M., Arnold, J. & Arabi, M. 2007 A hydrologic/water quality model application protocol. *Journal of the American Water Resources Association* **43** (5), 1223–1236. https://doi.org/10.1111/j.1752-1688.2007.00105.x.

Falchetta, G., Gernaat, D. E. H. J., Hunt, J. & Sterl, S. 2019 Hydropower dependency and climate change in sub-Saharan Africa: a nexus framework and evidence-based review. *Journal of Cleaner Production* **231**, 1399–1417. https://doi.org/10.1016/j.jclepro.2019.05.263.

Falchetta, G., Kasamba, C. & Parkinson, S. C. 2020 Monitoring hydropower reliability in Malawi with satellite data and machine learning. *Environmental Research Letters* **15** (1), 14011. https://doi.org/10.1088/1748-9326/ab6562.

Fitzsimmons, P. J. & Getoor, R. K. 2003 Homogeneous random measures and strongly supermedian kernels of a markov process. *Electronic Journal of Probability* **8** (2000), 1–54. https://doi.org/10.1214/EJP.v8-142.

Gagniuc, P. A. 2017 *Markov Chains: From Theory to Implementation and Experimentation*. John Wiley & Sons, Hoboken, New Jersey.

Gebrechorkos, S. H., Hülsmann, S. & Bernhofer, C. 2019 Regional climate projections for impact assessment studies in East Africa. *Environmental Research Letters* **14** (4). https://doi.org/10.1088/1748-9326/ab055a

Gordon, N. & Shaykewich, J. 2009 Guidelines on performance assessment of public weather services on performance assessment. *Technical Document* **1023**. Available from: https://www.wmo.int/pages/prog/amp/pwsp/qualityassuranceverification_en.htm

Hagemann, S., Chen, C., Clark, D. B., Folwell, S., Gosling, S. N., Haddeland, I., Hanasaki, N., Heinke, J., Ludwig, F., Voss, F. & Wiltshire, A. J. 2013 Climate change impact on available water resources obtained using multiple global climate and hydrology models. *Earth System Dynamics* **4** (1), 129–144. https://doi.org/10.5194/esd-4-129-2013.

Hamududu & Killingtveit, Å. 2010 Estimating effects of climate change on global hydropower production. In *Hydropower'10, 6th International Conference on Hydropower, Hydropower Supporting Other Renewables*, 1–3 February 2010, April, 13, Tromsø, Norway.

Hamududu, B. & Killingtveit, A. 2012 Assessing climate change impacts on global hydropower. *Energies* **5** (2), 305–322. https://doi.org/10.3390/en5020305.

Hasan, M. M. & Wyseure, G. 2018 Impact of climate change on hydropower generation in Rio Jubones Basin, Ecuador. *Water Science and Engineering* **11** (2), 157–166. https://doi.org/10.1016/j.wse.2018.07.002.

Hu, Z., Ni, Y., Shao, H., Yin, G., Yan, Y. & Jia, C. 2013 Applicability study of CFSR, ERA-Interim and MERRA precipitation estimates in Central Asia. *Arid Land Geography* **36**, 700–708.

Hwang, B. S. & Yoo, S. H. 2016 Electricity consumption and economic growth in Nicaragua. *Energy Sources, Part B: Economics, Planning and Policy* **11** (8), 746–752. https://doi.org/10.1080/15567249.2013.781247.

IHA. 2018 Advancing Sustainable Hydropower. *Currents IHA World Congress Magazine*, *1*.

Japan International Cooperation Agency 2011 *Guideline and Manual for Hydropower Development Vol. 1-Conventional Hydropower and Pumped Storage Hydropower* (March 2011). https://openjicareport.jica.go.jp/pdf/12024881_01.pdf.

Jiang, S., Ren, L. & Hong, Y. 2012 Comprehensive evaluation of multi-satellite precipitation products with a dense rain gauge network and optimally merging their simulated hydrological flows using the Bayesian model averaging method. *Journal of Hydrology* **452-453**, 213–225.

Jin, J., Wang, G., Zhang, J., Yang, Q., Liu, C., Liu, Y., Bao, Z. & He, R. 2018 Impacts of climate change on hydrology in the Yellow River source region, China. *Journal of Water and Climate Change* 1–15. https://doi.org/10.2166/wcc.2018.085.

Khare, D., Patra, D., Mondal, A. & Kundu, S. 2017 Impact of landuse/land cover change on run-off in the catchment of a hydro power project. *Applied Water Science* **7** (2), 787–800. https://doi.org/10.1007/s13201-015-0292-0.

Kizza, M., Rodhe, A. & Xu, C. 2009 *Temporal Rainfall Variability in the Lake Victoria Basin in East Africa During Temporal Rainfall Variability in the Lake Victoria Basin in East Africa During the Twentieth Century*. June 2014. https://doi.org/10.1007/s00704-008-0093-6.

Krapp, M., Beyer, R. & Manica, A. 2019 A systematic comparison of bias correction methods for paleoclimate simulations. *Climate of the Past Discussions.* **Feb 2019**, 1–23. https://doi.org/10.5194/cp-2019-11.

Langat, P. K., Kumar, L. & Koech, R. 2017 Temporal variability and trends of rainfall and streamflow in Tana River Basin, Kenya. *Sustainability* **9** (11). https://doi.org/10.3390/su9111963.

Li, Z., Yang, D. & Hong, Y. 2013 Multi-scale evaluation of high-resolution multi-sensor blended global precipitation products over the Yangtze river. *Journal of Hydrology* **500**, 157–169.

Lofthouse, J., Simmons, R. T. & Yonk, R. M. 2011 Reliability of renewable energy: geothermal. https://www.usu.edu/ipe/wpcontent/uploads/2015/11/Reliability-Geothermal-Full-Report.pdf.

Luhunga, P., Botai, J. & Kahimba, F. 2016 Evaluation of the performance of CORDEX regional climate models in simulating present climate conditions of Tanzania. *Journal of Southern Hemisphere Earth Systems Science* **66** (1), 32–54. https://doi.org/10.22499/3.6601.005.

Lv, X., Zuo, Z., Ni, Y., Sun, J. & Wang, H. 2019 The effects of climate and catchment characteristic change on streamflow in a typical tributary of the Yellow River. *Scientific Reports* **9** (1), 1–10. https://doi.org/10.1038/s41598-019-51115-x.

Masanganise, J., Chipindu, B., Mhizha, T., Mashonjowa, E. & Basira, K. 2013 An evaluation of the performances of Global Climate Models (GCMs) for predicting temperature and rainfall in Zimbabwe. *IJSRP* **3** (8), 1–11.

Mehrotra, R. & Sharma, A. 2015 Correcting for systematic biases in multiple raw GCM variables across a range of timescales. *Journal of Hydrology* **520**, 214–223. https://doi.org/10.1016/j.jhydrol.2014.11.037.

Ministry of Energy and Minerals Development. 2015 Uganda's Sustainable Energy For All (SE4All) Initiative Action Agenda. *Uganda's Sustainable Energy for All Initiative*, *June*, 1–78.

Moriasi, D. N., Arnold, J. G., Liew, M. W. V., Bingner, R. L., Harmel, R. D. & Veith, T. L. 2007 Soil water assessment tool: model use, calibration, and validation. *Transactions of the ASABE* **50** (3), 885–900.

Mutenyo, I., Nejadhashemi, P. A., Woznicki, A. S. & Giri, S. 2011 Evaluation of SWAT performance on a mountainous watershed in tropical Africa. *Hydrol. Current Res.* **s3**, 1–7. https://doi.org/10.4172/2157-7587.s14-001.

Näschen, K., Diekkrüger, B., Evers, M., Höllermann, B., Steinbach, S. & Thonfeld, F. 2019 The impact of land use/land cover change (LULCC) on water resources in a tropical catchment in Tanzania under different climate change scenarios. *Sustainability* **11** (24). https://doi.org/10.3390/su11247083.

Ndhlovu, G. Z. & Woyessa, Y. E. 2020 Modelling impact of climate change on catchment water balance, Kabompo River in Zambezi River Basin. *Journal of Hydrology: Regional Studies* **27**, 100650. https://doi.org/10.1016/j.ejrh.2019.100650.

Ndulue, E. L., Mbajiorgu, C. C., Ugwu, S. N., Ogwo, V. & Ogbu, K. N. 2015 Assessment of land use/cover impacts on runoff and sediment yield using hydrologic models: a review. *Journal of Ecology and The Natural Environment* **7** (2), 46–55. https://doi.org/10.5897/jene2014.0482.

Neitsch, S., Arnold, J., Kiniry, J. & Williams, J. 2011 *Soil & Water Assessment Tool Theoretical Documentation Version 2009*. Texas Water Resources Institute, pp. 1–647. https://doi.org/10.1016/j.scitotenv.2015.11.063.

Othow, O. O., Gebre, L. S. & Obsi, G. D. 2017 Analyzing the rate of land use and land cover change and determining the causes of forest cover change in Gog District, Gambella Regional State, Ethiopia. *Journal of Remote Sensing & GIS* **6** (4). https://doi.org/10.4172/2469-4134.1000219.

Pokhrel, P., Ohgushi, K. & Fujita, M. 2019 Impacts of future climate variability on hydrological processes in the upstream catchment of Kase River basin, Japan. *Applied Water Science* **9** (1), 1–10. https://doi.org/10.1007/s13201-019-0896-x.

Puno, R. C. C., Puno, G. R. & Talisay, B. A. M. 2016 Hydrologic responses of watershed assessment to land cover and climate change using soil and water assessment tool model ARTICLE INFO. *Global Journal of Environmental Science and Management* **5** (1), 71–82. https://doi.org/10.22034/gjesm.2019.01.06.

Rathjens, H., Bieger, K., Srinivasan, R., Chaubey, I. & Arnold, J. 2016 Documentation for preparing simulated climate change data for hydrologic impact studies. https://swat.tamu.edu/media/115265/bias_cor_man.pdf.

Roudier, P., Ducharne, A. & Feyen, L. 2014 Climate change impacts on runoff in West Africa: a review. *Hydrology and Earth System Sciences* **18** (7), 2789–2801. https://doi.org/10.5194/hess-18-2789-2014.

Rugumayo, A., Taylor, T., Markandya, A. & Droogers, P. 2014 Economic assessment of the impacts of climate change in Uganda. *Costume* **8** (1), 61. https://doi.org/10.1179/cos.1974.8.1.61.

Santhi, C., Arnold, J. G., Williams, J. R., Dugas, W. A., Srinivasan, R. & Hauck, L. M. 2001 Validation of the SWAT model on a large river basin with point and nonpoint sources. *J. Am. Water Resour. Assoc.* **37** (5), 1169–1188.

Searcy, K. J. 1959 *Flow Duration Curve. Manual of Hydrology: Part 2. Low-Flow Techniques.* https://pubs.usgs.gov/wsp/1542a/report.pdf.

Singh, J., Knapp, H. V. & Demissie, M. 2004 *Hydrologic Modeling of the Iroquois River Watershed Using HSPF and SWAT. ISWS CR 2004–08*. Illinois State Water Survey, Champaign, IL, USA. www.sws.uiuc.edu/pubdoc/CR/ISWSCR2004-08.pdf.

Sun, L., Hao, Z., Wang, J., Nistor, I. & Seidou, O. 2014 Assessment and correction of TMPA products 3B42RT and 3B42v6. *Shuili Xuebao* **46**, 1135–1146.

Todd, M. C., Andersson, L., Ambrosino, C. & Hughes, D. A. 2011 *Climate Change Impacts on Hydrology in Africa: Case Studies of River Basin Climate Change Impacts on Hydrology in Africa: Case Studies of River Basin (Issue January 2015)*. https://doi.org/10.1007/978-90-481-3842-5.

Treesa, A., Das, J. & Umamahesh, N. V. 2017 Assessment of impact of climate change on streamflows using VIC model. *European Water* **59** (2013), 61–68.

Uamusse, M. M., Aljaradin, M. & Persson, K. M. 2017 Micro-hydropower plant – energy solution used in rural areas, Mozambique. *Sustainable Resources Management* **1**, 3–9.

UEGCL 2013a *Consultancy Services for Feasibility Study of Muzizi Hydropower Project*. Vol. 1, September.

UEGCL 2013b *Consultancy Services for Feasibility Study of Muzizi Hydropower Project FEASIBILITY STUDY REPORT*. Vol. 1, September.

USGS 2020 *Landsat Data Access. United States Geological Survey.* http://landsat.usgs.gov/Landsat_Search_and_Download.php.

van Liew, M. W., Arnold, J. G. & Garbrecht, J. D. 2003 Hydrologic simulation on agricultural watersheds: choosing between two models. *Transactions of the ASAE* **46**, 1539–1551.

Veldkamp, A. & Lambin, E. F. 2001 Editorial: predicting land-use change. *Agriculture, Ecosystems and Environment* **85** (1–3), 1–6. https://doi.org/10.1016/S0167-8809(01)00199-2.

Wang, Z., Lin, L., Zhang, X., Zhang, H., Liu, L. & Xu, Y. 2017 Scenario dependence of future changes in climate extremes under 1.5°C and 2°C global warming. *Scientific Reports* **7**, 1–9. https://doi.org/10.1038/srep46432.

Welde, K. & Gebremariam, B. 2017 Effect of land use land cover dynamics on hydrological response of watershed: case study of Tekeze Dam watershed, northern Ethiopia. *International Soil and Water Conservation Research* **5** (1), 1–16. https://doi.org/10.1016/j.iswcr.2017.03.002.

Zhang, L., Nan, Z., Xu, Y. & Li, S. 2016 Hydrological impacts of land use change and climate variability in the headwater region of the Heihe River Basin, northwest China. *PLoS ONE* **11** (6). https://doi.org/10.1371/journal.pone.0158394.

Zhu, Z., Shi, C., Zhang, T., Zhu, C. & Meng, X. 2015 Applicability analysis of various reanalyzed land surface temperature datasets in China. *Journal of Glaciology and Geocryology* **37**, 614–624.

Zuo, D., Xu, Z., Yao, W., Jin, S., Xiao, P. & Ran, D. 2016 Assessing the effects of changes in land use and climate on runoff and sediment yields from a watershed in the Loess Plateau of China. *Science of the Total Environment* **544**, 238–250. https://doi.org/10.1016/j.scitotenv.2015.11.060.

First received 6 September 2020; accepted in revised form 21 March 2021. Available online 8 April 2021